THE EFFECT OF TEMPERATURE AND RELATIVE HUMIDITY ON THE CORROSION RATES OF COPPER AND SILVER IN ELECTRONIC EQUIPMENT IN THE PRESENCE OF SULFUR ENVIRONMENT

By

KANAN PUJARA

Presented to the Faculty of the Graduate School of

The University of Texas at Arlington in Partial Fulfillment

of the Requirements

for the Degree of

MASTER OF SCIENCE IN MECHANICAL ENGINEERING

THE UNIVERSITY OF TEXAS AT ARLINGTON

December 2015

Acknowledgements

I would like to take this opportunity to thank my thesis guide Dr. Dereje Agonafer, who was a source of inspiration to me throughout my work. The experimental work presented here was performed at IBM facility, Poughkeepsie and it was because of Dr. Agonafer that I could get such an opportunity and his encouragement to help me cross all the obstacles.

I would also like to thank Dr. Parabjit Singh, IBM who was my mentor and torch bearer for me in this project related to contamination in data centers. I got to learn many technical and non-technical skills from him during my tenure at IBM for a period of 2 months. I would also like to thank the lab employees at IBM who helped me for my experiments.

I would also like to thank Dr. Haji-Sheikh and Dr. Kent Lawrence for being on my thesis committee and helping me whenever I need a helping hand. A special thanks to Ms. Sally Thompson for her immense help throughout my stay at UT Arlington. I would also like to thank my friends at the EMNSPC who were as good as my family across seas. My special thanks to my friend Devi Prasad, who was there to support and help me during my tough times.

Finally I would like to dedicate my thesis to my grandparents Late Mr. Premchand S. Pujara and Late Mrs. Sharda P. Pujara who made me what I am today and giving me the strength to prove myself, my parents Mr. Dinesh Pujara and Mrs. Sudha Pujara have always been my source of motivation, my brother Mr. Jay Pujara, my sister-in-law Mrs Bhumika Pujara, my nephews Yash Pujara and Rushi Pujara and my friend Tushar Saini for being with me and holding me in all the tough times and having faith in me and my work.

November 24, 2015

Abstract

THE EFFECT OF TEMPERATURE AND RELATIVE HUMIDITY ON THE CORROSION RATES OF COPPER AND SILVER IN ELECTRONIC EQUIPMENT IN THE PRESENCE OF SULFUR ENVIRONMENT

Kanan Pujara, MS

The University of Texas at Arlington, 2015

Supervising Professor: Dereje Agonafer

Data centers consume a significant amount of energy for the continuous air-conditioning of the servers with high internal heat loads and to maintain the indoor temperatures within recommended operating levels as recommended by ASHRAE. As an alternate source to air-conditioning, air-side economizers are used to reduce power consumption. Air-side economizers bring in large amounts of the outside free air to cool internal loads, when weather conditions are favorable, saving a considerable amount of energy by reducing chiller operation. However, there is a reluctance in using this technique due to undetermined equipment reliability by introducing outside air pollutants which over time could cause failures.

The ASHRAE TC 9.9 committee of IT equipment manufacturers published the 2008 ASHRAE Environmental Guidelines for Datacom Equipment extending the temperature-humidity envelope providing greater flexibility in data center facility operations with the goal of reducing energy consumption. There is a need to know the degree of reliability degradation when the equipment is operated, outside the recommended range, in the allowable temperature-humidity range in geographies with high levels of gaseous and particulate contamination. This research restricts itself to the effect of temperature and humidity on corrosion-related hardware failures, in sulfur-

bearing gaseous contaminated environments, by studying copper and silver corrosion rates as a function of temperature and humidity; the assumption being that the frequency of occurrence of corrosion-related hardware failures is proportional to the copper and silver corrosion rates.

The research presented here uses a technique of measuring the corrosion of a metal by the virtue of its electrical resistance. As the metal corrodes, its cross-sectional area reduces, hence increasing its electrical resistance. By continuously monitoring resistance, corrosion can be monitored in the controlled atmosphere where the wire is exposed. Though the technique is simple in principle, there are a number of practical problems to be considered while using it in electronic equipment when applied to atmospheric corrosion tests.

An ASHRAE survey of data centers has shown that there is a strong relationship of corrosion-related hardware failure frequency to copper and silver corrosion rates under various temperature and relative humidity ranges. The gaseous contamination is provided in the form of approximately 70 ppb free sulfur in a flowers of sulfur (FOS) chamber maintained at 30°C constant temperature. The humidity in the FOS chamber is maintained at various levels by using saturated salt solutions and the thin film temperature is maintained at various levels between 30 and 50°C by the joule heating of the films. The corrosion rates of copper and silver, in a 30°C ambient with ~70 ppb free sulfur, are plotted in the upper right corner of the ASHRAE A1-A4 allowable temperature-humidity ranges. For the first time, corrosion data are provided on the psychrometric chart in a form convenient for obtaining the x-factors for temperature and humidity for corrosion-related hardware failures.

Table of Contents

List of Illustrations

List of Tables

Chapter 1

Introduction

A Data Center is a central repository of an IT Equipment used for processing, storing and exchanging digital information. The brain of data center is the server where the processes takes place. These servers are mounted in a standardized cabinets called rack. These racks of servers constitute the IT equipment and the main frame of data center. The neural system of the data center is the supporting equipment providing uninterrupted power and cooling. The Heating, Ventilation and Air Conditioning (HVAC) provides the necessary cooling to maintain the required temperatures. Thus, power consumptions by the data center for its continuous operation is very high.

With the intention to foster a better alignment between equipment manufacturers and facility operations, the American Society for Heating Refrigeration and Air Conditioning Engineers (ASHRAE) TC 9.9 Committee has developed certain guidelines for design, operation, maintenance, and efficient energy usage of modern data centers. The objective is to identify and spread best practices to data center administrators. The recommended temperature limits are from 18°C (64.4°F) to 27°C (80.6°F). The humidity is limited to less than 60% with the lower and upper dew point temperatures of 5.5°C (41.9°F) and 15°C (59°F) [1]. The ASHRAE TC 9.9 committee of IT equipment manufacturers published the 2008 ASHRAE Environmental Guidelines for Datacom Equipment extending the temperature-humidity envelope providing greater flexibility in data center facility operations with the goal of reducing energy consumption. A downside of expanding the temperature-humidity envelope is the reliability risk from higher levels of gaseous and particulate contamination entering the data center.

1.1 Energy usage and cooling alternatives

Increasing dependence on computer based application has led to the demand for faster and improved communication. Humans have a never-ending desire to store the data in multiple forms and possess copies, no matter where they are, whether in offices, or travelling, has given rise to the use of microelectronic devices (MCD) integrated with microelectromechanical systems (MEMS). Throughout global demand and tough competition between competitors, these products needs to be produced at decreasing costs and improved reliability. According to the Moore's law, the processor speed, or the overall processing power doubles every two years. In order to match with the rising demands, better and efficient computing devices are needed for information processing which has eventually led to the growth of datacenters. A significant amount of energy is utilized for the continuous air-conditioning of the servers with high internal heat loads and to maintain the indoor temperatures within recommended operating. Rising energy costs and ever growing needs for power supplies worldwide has led to increasing efficient use of energy. Due to the recent climatic changes and the greenhouse effect has generated focus on energy savings and use of alternate sources of energy.

The data reported by Koomey mentions that the server electrical use alone represents 1.2% of U.S. electrical use and close 2% for overall electrical use of data center in US [2]. His study stated that the server electrical use has doubled from 2000 to 2005 and will grow by 15% annually from 2006 to 2010. Other articles and references have detailed similar growth rates at individual firms. This rapid increase in energy usage has attracted the attention of environmental agencies in the U.S., European Union, China and other countries. In order to meet with the rising computing costs for the data centers, practices are implementing for cost-cutting measures like operating slightly above the recommended envelope and using the outside ambient air.

The ASHRAE TC9.9 subcommittee, on Mission Critical Facilities, Data Centers, Technology Spaces, and Electronic Equipment, has accommodated the data center administrators by allowing short period excursions outside the recommended temperature-humidity range, into allowable classes A1-A4. Under worst case conditions, the ASHRAE A3 envelope allows electronic equipment to operate at temperature and humidity as high as 24˚C and 85% relative humidity for short, but undefined periods of time [3]. Any choice outside of the recommended region will be a balance between the additional energy savings of the cooling system versus the deleterious effects that may be created in reliability, acoustics, or performance [4]. Various cost-cutting alternatives such as not tightly controlling the temperature and relative humidity levels or using an Air-Side Economizers are implemented, keeping in mind the associated risk of allowing the particulate and gaseous contaminants into their data centers.

Power usage effectiveness (PUE) has become the new metric to measure data center efficiency which creates a measurable way to see the effect of data center design and operation on data center efficiency. To improve PUE, air- and water-side economization have become more commonplace with a drive to use them year round. To enable improved PUE capability, TC 9.9 has created additional environmental classes along with guidance on the usage of the existing and new classes. Expanding the capability of IT equipment to meet wider environmental requirements can change reliability, power consumption and performance capabilities of the IT equipment and guidelines are provided herein on how these aspects are affected [5].

Alternate sources to air-conditioning, air-side economizers are used to reduce power consumption. The air-side economizers work on the principle of free air cooling which implements outside ambient air as the working fluid. Figure 1-1 shows the

schematics of an air-side economizer while Figure 1-2 shows the working of an air-side economizer.

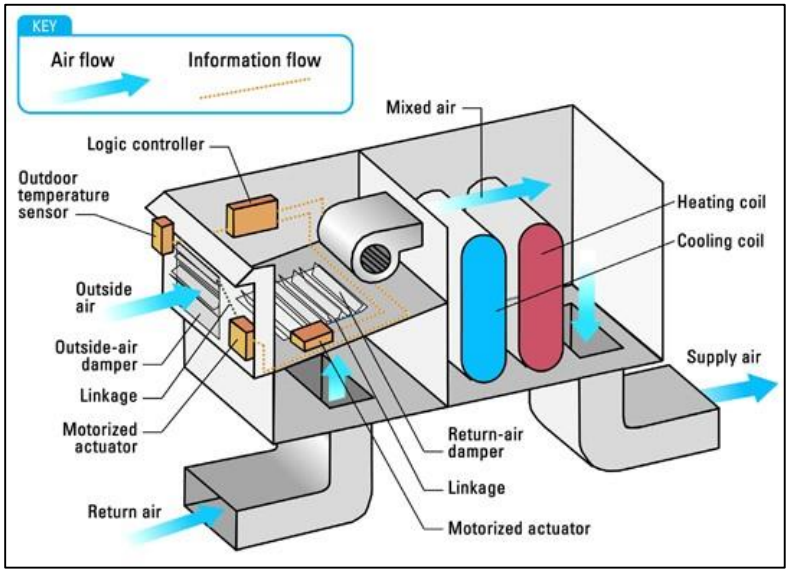

Figure 1-1 Air-side Economizer

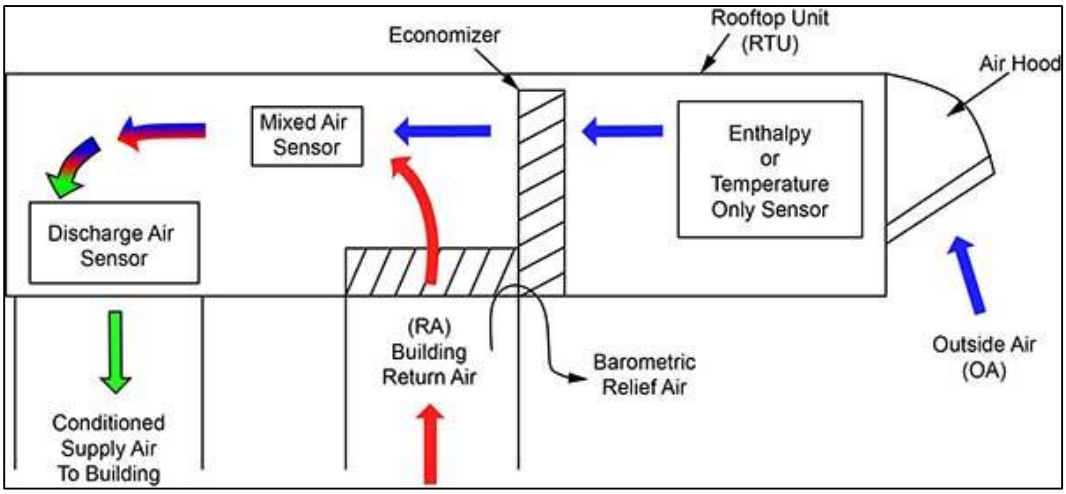

Figure 1-2 Working of an air-side economizer

Air-side economizers bring in large amounts of the outside free air to cool internal loads, when weather conditions are favorable, saving a considerable amount of energy by reducing chiller operation [6]. Instead of cooling the recirculated, the hot (exhaust) air from the servers is simply directed to the atmosphere. When the outside air is at a lower temperature then the recirculated inside air, the economizer mixes it with the hot (exhaust) air to achieve the desired range of temperature and humidity. With proper filtration and conditioning, the mixed air is then supplied to the datacenter. But when the outside air is both sufficiently cool and dry (depending on the climate) the amount of enthalpy in the air is acceptable and no additional conditioning of it is needed; this portion of the air-side economizer control scheme is called *free cooling* [7].

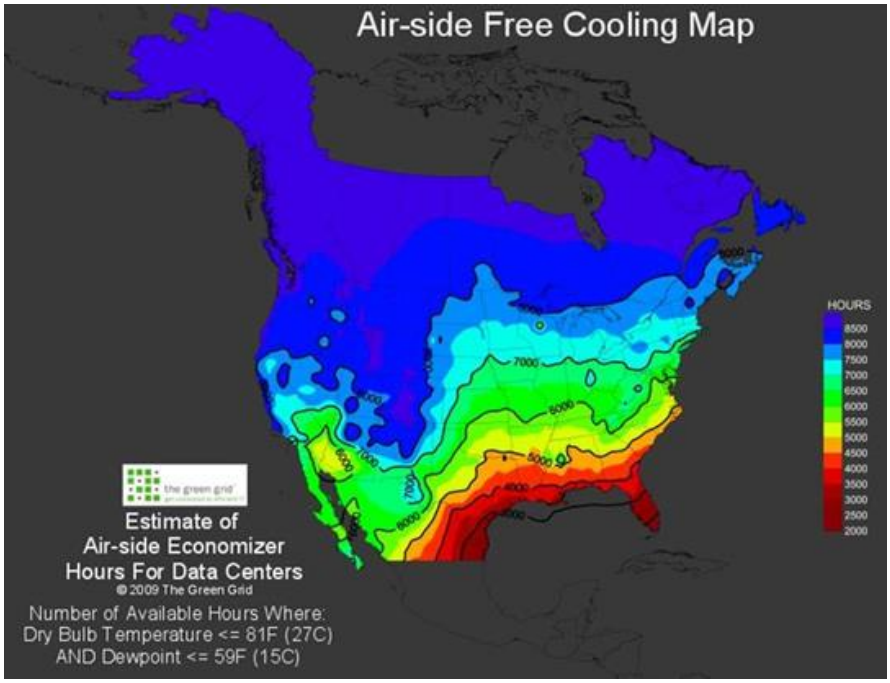

Figure 1-3 Hours with ideal conditions for an air-side economizer

(Image source: [7])

The air-side economizer is introjected into the central air handling system for intake and exhaust air, with suitable filters to reduce the particulate matter or contaminants entering the data center. Many datacenters across the U.S. take the benefit of this free cooling. Figure 1-3 shows the usage of air-side economizers in hours per year. The associated risk of impurities entering the datacenter is discussed in next chapter.

1.2 Contamination in Datacenters

Datacenters are well designed and are placed in a suitable and relatively clean environments. Hence they do not experience any particulate and gaseous contamination, and if experienced, it is relatively benign. The work presented here is focused on those small fraction of datacenters which have harsh and harmful environmental conditions that is mainly due to particulate and/or gaseous contaminants. Intel IT conducted a proof-of-concept test that used an air-side economizer to cool servers with 100% outside air at temperatures of up to 90°F. A survey conducted by them estimates that a 500kW facility will save $144,000 annually and that a 10MW facility will save $2.87 million annually [8]. However, this technology is not widely adopted because of many factors like the class of environment (temperature variations) in which economizers are placed, climatic conditions (exg. humid to dry air conditions). The reluctance in using this technique is due to the undetermined equipment reliability due to introduction of outside air pollutants which over time could cause failures. It should also be noted that the reduction of circuit board feature sizes and the miniaturization of components, necessary to improve hardware performance, also makes the hardware more prone to attack by the corrosive particles and gases in the data center environment. This develops the need to study the detrimental effects of using free cooling on the IT equipment reliability.

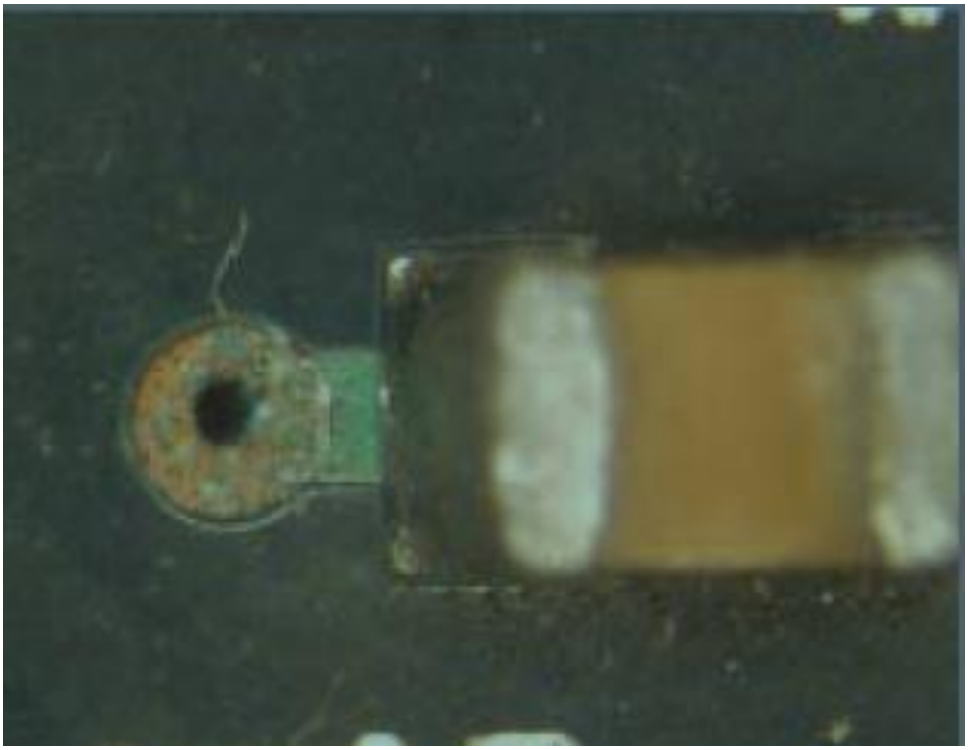

Figure 1-4 Corrosion of a plated through hole because of wetted ionic dust

(Image Source: [4])

Expansion in the ASHRAE's guidelines for data center safe operating temperature-humidity envelopes generates the need to know the potential risk or predicting the failure rates of hardware that is involved in operating outside the envelopes. The recommended range for temperature as given by ASHRAE is 18ºC to 27ºC and for humidity is up to 60%. These conditions are conducive enough for corrosion to occur on the IT equipment. Thus, the air entering the datacenter via the economizers pose a potential threat to electronics of the IT equipment. Hence, any choice outside of the recommended region should be a balance between the additional energy savings of the cooling system versus the deleterious effects that may be created in reliability, acoustics, or performance [4].

Various particulate matters like pollen, dust, debris, automobile emission, carbon dust, smoke, etc. are known to enter the datacenter. Specially designed MERV filters are used to filter the particulates but the ones with diameter < 2.5μm are reported to be unfiltered. These particulate matter (PM) is known to become wet under the influence of moisture present and therefore becomes conductive. When the deliquescence relative humidity (DRH) of the particulate matter is lower than that of the relative humidity of datacenter, the PM gets wet by absorbing water and becomes corrosive in nature [9]. Figure 1-4 is an example of copper corrosion caused by dust settled on a printed circuit board.

While the PM is wet results in electrically bridging closely spaced features on printed circuit boards, resulting in current leakage eventually leading to their electrical failure [3]. According to ISA-71.04-1985, “Failures attributed to particulate matter have even been observed in data centers where the gaseous contamination levels are low enough to meet the ANSI/ISA-71.04-2013 G1 severity level” [10] . Thus with the miniaturization of electronic components, the reduction of feature spacing on PCBs along with the loosening of the data center temperature and humidity envelope to save energy is making electronic hardware more prone to failure due to particulate matter [3]. The role of gaseous contamination is discussed in next chapter.

1.3 Gaseous Contamination

With the increase in the rate of hardware failures in data centers high in sulfur-bearing gases, led to the study of dust and gaseous contamination. Corrosion induced failures is common in electronics due to higher levels of gaseous contaminations. Common modes of corrosion failures due to gaseous contamination is are the corrosion of silver terminated surface mount resistors and the creep corrosion on printed circuit boards (PCBs) [11]. The corrosion of silver terminations in the Surface Mount Technology (SMT) resistors has been brought largely under control by improving the packaging of the resistors. The creep corrosion of PCBs is believed to be more susceptible to RoHS complaint circuit boards [12] [13]. RoHS is the European Union of Restriction of Hazardous Substance (RoHS) directive issued in February 2003 that took effect on 1 July 2006, banning the use of lead in solder joints [14].

According to ASHRAE TC 9.9, “the silver and copper solder contained the lead tin (PbSn) solder has two shortcomings: One is its higher melting range that necessitates the change of PCB laminate epoxies to ones with higher glass transition temperatures; the second is the poor wetting of the copper metallization on the PCBs by the lead-free solder, necessitating the use of various surface finishes on the copper metallization to enhance wetting by the lead-free solder”. The net result is that the RoHS compliant PCBs are more prone to creep corrosion as shown in Figure 1-5 [11]. Picture courtesy 2011 “Gaseous and Particulate Contamination Guidelines for Data Centers”.

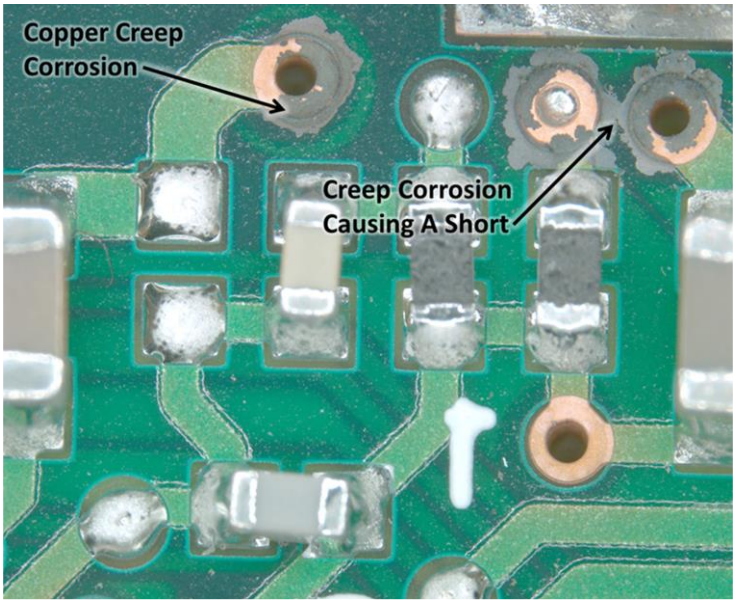

Figure 1-5 Example of copper creep corrosion on a lead-free circuit board

(Image source: [4])

Creep corrosion is the corrosion of copper (and sometimes silver) metallization on PCB and creeping the corrosion product, mainly the sulfides, resulting in the electrical shorting of PCBs. From the survey by Fu, H., Zhou, Y. et al, the challenge still remains to develop a reliable qualification test for creep corrosion, though progress has been made developing the mixed flowing gas (MFG), the Chavant clay and the flowers of sulfur tests [12] [13] [15]. The gaseous contaminants when enters the datacenter, under the influence of temperature and humidity, undergo a chemical reaction with the elements of PCB resulting in the surface deposition of products like oxides, sulfides or chlorides. These products gradually increase and short circuit the adjacent buses or solder joints as shown in Figure 1-6 and Figure 1-7

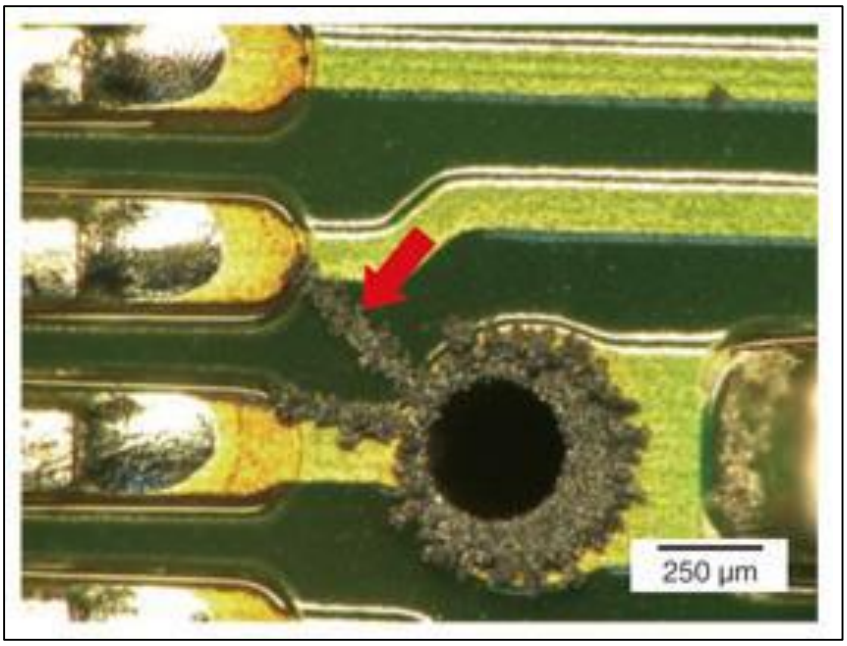

Figure 1-6 Short in adjacent solder hole and bus line as a result of surface deposition

(Image source: [16])

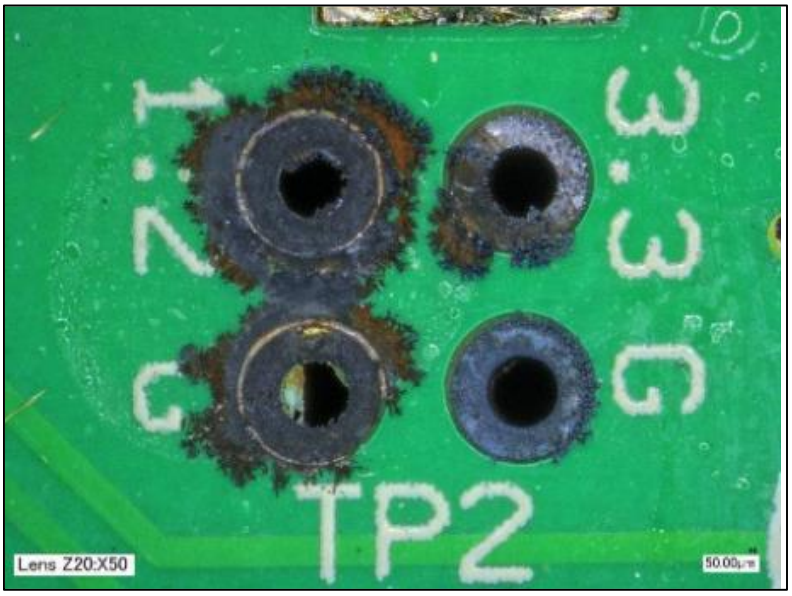

Figure 1-7 Short Due to the Mixture of Gaseous Contaminants

(Image source: [12])

Sulfur bearing gases, such as Sulfur dioxide (SO_2) and Hydrogen sulfide (H2S), are the most common gases in the datacenter causing hardware corrosion [17]. Other harmful gases like, Nitrogen dioxide (NO2) and Chlorine (Cl2) are also considered to have the most influence on the corrosion of copper and silver. Gaseous composition environmental limits have been published in ANSI/ISA-71.04-1985 [18]. Determination of gaseous composition is not trivial. The gaseous composition present in the air can be determined using a gas analyzer. Predicting the rate of corrosion from the synergy of various gases becomes a complicated task. A low-cost, simple approach to monitoring the air quality in a data center is to expose copper and silver foil coupons in the data center for 30 days followed by coulometric reduction analysis in a laboratory to determine the thickness of the corrosion products on the metal coupons [19]. From a survey of ASHRAE literatures and whitepaper, it is observed that a very strong relationship for the frequency of corrosion related hardware failures to the copper and silver corrosion rates [18].

1.4 Copper and Silver Corrosion

Copper and silver are important functional metals used widely in electronics industry worldwide. Copper and its alloys are widely applied in the electric energy, electronics, and semiconductor industries because of its properties of high electrical and thermal conductivity, ductility, and malleability. Corrosion of both copper and silver is a common problem and has been studied extensively. The atmospheric corrosion process is more complex than oxidation at high temperatures [20]. There is no such theory that exists for atmospheric corrosion, although attempts have been made to correlate observed outdoor rates to sulfate and relative humidity levels [21]. Water vapor, sulfur dioxide, and hydrogen sulfide have been shown to influence the rate of copper corrosion

[22] [23]. Silver has been cited as a classical example of a material that decays by a diffusion-controlled process at either the atmosphere-product interface or in the corrosion product itself [24]. Sulfur gases are the dominant reactive pollutants [25] [26]; however, some reference is given to humidity and chlorine-containing gases as accelerators of corrosion [27] [28].

Corrosion is a complex process that changes the surface properties, even at ambient temperature, forming a thin layer having completely different properties compared with the pure metal surface. This layer lowers catastrophically the adhesion of the soldering alloy or conductive resins and paste, provoking failures of the printed circuit board (PCB) of the microelectronic devices. The formation of tarnish films on a copper surface exposed to environments containing atmospheric pollutants and high humidity involves the movement of metallic ions over the surface, away from the metal generating a creep process that increases the contact resistance, leading to electric failures of the electronic devices [29]. Copper sulphidation is a fast process occurring on the metal-gas phase interface impairing the copper corrosion resistance [30] [31]. It is important to add to the understanding the complex chemistry of copper and silver corrosion under varied conditions of temperature and humidity. We develop the quantitative rate dependence on relative humidity and pollutant concentrations in laboratory.

1.5 Motivation

As discussed earlier in Ch.1.3, changes to electronic equipment due to the RoHS compliance required the elimination of lead in electronic equipment. Due to this, the PCBs which are lead-free are now more susceptible to corrosion related failures then their tin/lead counterparts. This means that the environment previously considered to be benign for electronics corrosion are now experiencing serious corrosion related failure of

IT equipment [32] . With the introduction of a number of regulations by RoHS and the switch to lead-free finishes, there is a need to develop a monitoring technique for this type of environment. Reactive monitoring now needs to provide a complete and a better assessment for the changing environmental conditions rather than the monitoring techniques described in ISA implementations of RoHS.

Also, due to the expansion in the ASHRAE's recommended envelope to allowable envelopes A1 to A4 as shown inFigure 1-8, there is a need to know the reliability degradation when the equipment operates outside the recommended range in the allowable temperature-humidity range in geographies with high levels of gaseous and particulate contamination. Understanding the corrosion chemistry using only copper would give insufficient information. Copper has two limitations, one is its insensitivity to chlorine, a contaminant particularly corrosive to many metals, and another is that copper corrosion is highly sensitive to relative humidity. The inclusion of a silver coupon helps contributions of gaseous contaminations and relative humidity.

A very common practice now is to include silver coupons along with copper coupons to gain greater insight into the chemistry of the corrosive gases in the environment. This work restricts itself to the effect of temperature and humidity on corrosion-related hardware failures, in sulfur-bearing gaseous contaminated environments, by studying copper and silver corrosion rates as a function of temperature and humidity; the assumption being that the frequency of occurrence of corrosion-related hardware failures is proportional to the copper and silver corrosion rates.

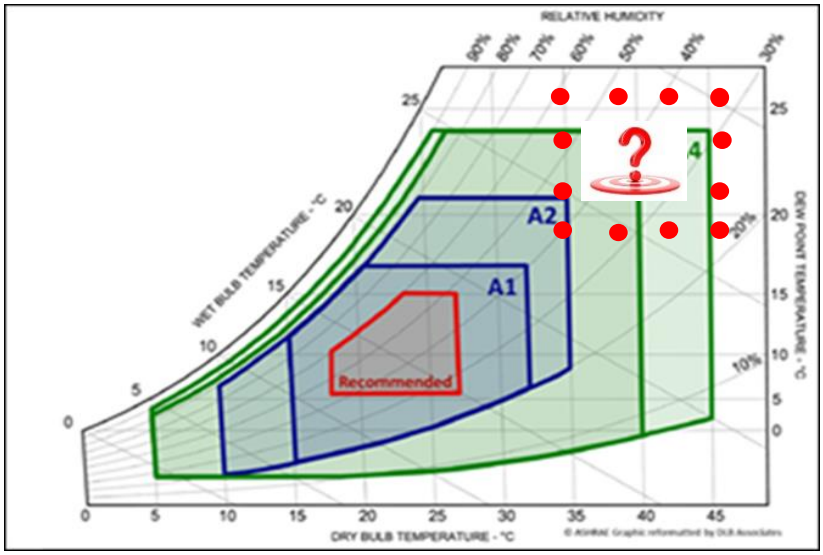

Figure 1-8 Recommended and allowable environmental conditions for electronic equipment

(Image source: ASHRAE, 2012 3rd edition)

The scope of this work is to find the effect of temperature and relative humidity on the Corrosion rate of Copper and Silver outside the recommended range (i. e. in the allowable range). This main objective of this research is to develop a test to predict the reliability of the hardware while operating outside the recommended range in geographies with high levels of contamination. This research will benefit industry with a reliable, low-cost corrosion qualification test which could be used to find the impact of various test conditions to predict the product reliability under harsh environments and various geographies contaminated with sulfur-bearing gases. Datacenter administrators can now make calculated risqué as when to operate outside the recommended zone and use free-cooling for additional energy savings and yet not degrade the equipment reliability and electrical performance. As a result of this research, for the first time ever, corrosion rates of copper and silver would be provided on the psychrometric chart.

Chapter 2

Experimental Set-up

The main idea for this experiment is to simulate the real world data center conditions, i.e. the physical environment surrounding the IT equipment like temperature and relative humidity and the gaseous and airborne impurities, inside the laboratory. Environmental durability must be designed into the electronics which is often exposed to harsh and extreme weather conditions. To observe and quantify the effect of the environmental pollutants on the printed circuit boards (PCB) i.e. predominantly on the copper and silver metal, it is placed in a chamber and exposed to a pollutant containing environment and allowed to corrode under various temperature and relative humidity conditions.

2.1 Approach

To obtain reproducible and meaningful test results for the components under tests in laboratory require careful calibration and monitoring is very crucial. Ideally, a calibration and monitoring technique should be simple, accurate and continuous in order to provide useful information promptly, efficiently. The experiment should be easily reproducible. Changes in resistance of metallic conductors has been used especially when the conductors are copper paths on printed circuit boards [33]. These monitors are relatively easy to handle. The technique used here is by measuring the corrosion of a metal wire by the virtue of its electrical resistance. As the metal wire corrodes, its cross-sectional area reduces, hence increasing its electrical resistance. By continuously monitoring resistance, corrosion can be monitored in the controlled atmosphere where the wire is exposed. Though the technique is simple in principle, there are a number of practical problems to be considered while using it in electronic equipment when applied

to atmospheric corrosion tests. These problems include (a) the need to use very small diameter wire which are quite fragile, (b) the need to clean the wire in a reproducible and effective initialization process; and (3) the need to hold the wire in a resistance-measuring fixture without using solder and solder flux [34].

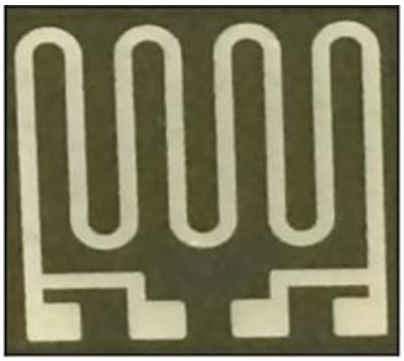

Figure 2-1 Silver Thin Film

To overcome this drawback, we have used the thin films of copper and silver as shown in chapter 2.2. These thin films are strong enough and satisfies the necessary properties for being used as a corrosion monitor. The advantage of using a thin film over a “reactive monitoring technique” by using a coupon is that the thin films can be calibrated in such a way that constant current can be supplied to it to undergo Joule’s heating or self-heating. The Joule’s Law of Heating (also referred as resistive or ohmic heating) is the energy produced is converted into heat as the current flowing through the conductor encounters resistance against it. The heat produced is proportional to the square of the amount of current flowing through the circuit, with constant electrical resistance and time of current flow. In particular, when the current flows through the solid with finite conductivity, electrical energy is converted to thermal energy through resistive losses in the material. The heat generated on the microscale when the conduction electrons transfer energy to the conductor’s atoms by way of collisions. The phenomenon of Joule’s heating a common problem in electronics industry.

2.2 Thin Films

In this experiment, thin films (thickness of the order in nanometers) of copper and silver metal is used as shown in Figure 2-1. The thickness of the copper and silver thin film is 1004.0 nm and 772.3 nm respectively as measured using KLA Tencor's ® step profile-o-meter at IBM York Town facility, NY. The copper and silver pattern is compressed on silicon layer of 0.5 mm thick. The length and width of the silicon vase is 15mm and corresponding surface area of the thin film is 225 mm^2. The thin films are stored in an air-tight container and stored in a dry space so that it is not exposed to slightest level of contamination. A series of process is being performed before the thin film is being used for the experiment. The serpentine profile of the copper and silver film was observed under microscope and the thickness and overall length of the profile was noted. The width of the film is 0.6572 mm while the equivalent length was 70.0 mm. These values are useful for the calculation of electrical resistivity of the metal.

2.3 Specimen Preparation

The corrosion of the metal is measured by the changes in the resistance when the metal is allowed to degrade under certain conditions, hence it is very necessary to make an accurate resistance measuring technique for this purpose. The most accurate way of resistance measurement is using a wheat-stone bridge. A wheat-stone bridge is the most accurate way of measuring the resistance across any electrical circuit. A 4-point Potentiostat is set by connecting four copper wires to the thin films. Current is supplied across the terminals and voltage at each levels is measured under different temperature and relative humidity. Resistance is calculated at each stage and corrosion rate is derived from it.

To ensure that no contamination occurs via human interface and human safety, eye-glasses, gloves, and lab-coat should be worn while performing the experiment. Care should be taken that no contaminants are introduced while handling it. To set-up a 4-point potentiostat, a glass slide is initially cleaned with Iso-Propane Alcohol (IPA) and distilled water to ensure that it is dust free. Once cleaned, it is dried using dry Nitrogen gas (N_2). Now the glass slide is clean enough for further use. Thereafter, a thermocouple is placed on the glass slide using a scotch tape. The thermocouple should be tested for its functionality before the wire is taped to the glass slide. The Epoxy-patch adhesive mixture is then placed uniformly around the periphery of thermocouple bead. The Epoxy-patch is prepared by mixing thoroughly equal quantities of Hardener and Resin paste. Thin films should be examined carefully under the electron microscope for the dust particles or any sort of damage before using it any further. Selected thin film is then bonded to the thermocouple and glass slide using the tweezer using epoxy. The epoxy-patch glued to the glass slide by keeping some weight initially like a spring loaded weight, taking care that the film doesn't break, and then allowed to set for 6-7 hours.

Next is to connect the copper wires to the thin films. Firstly, the current carrying capacity of the copper wire should be checked before using it. Also, the maximum temperature capacity of the copper-silver thin film should also be known to sustain and function properly. Two pairs of four copper wires each of equal length (equivalent to the half the chamber door size, i.e. 4 inches) should be connected with the single pin Berg connector. Each of these copper wires are fixed to single pin Berg connector and locked into its female 4-pin Berg connectors which will hold the four copper wires from thin film. Figure 2-2 and Figure 2-3 shows the various berg connectors used.

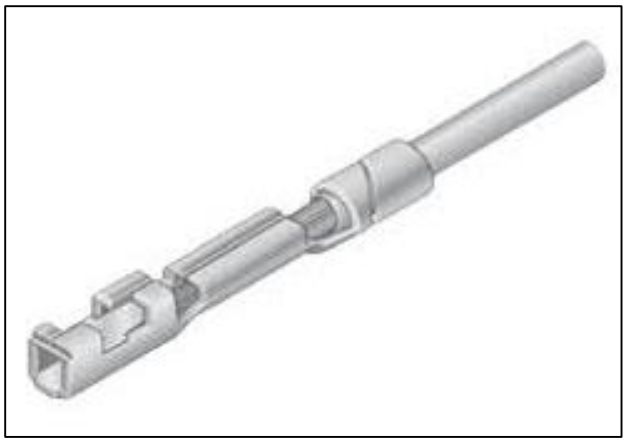

Figure 2-2 Single pin Berg connector (Male part)

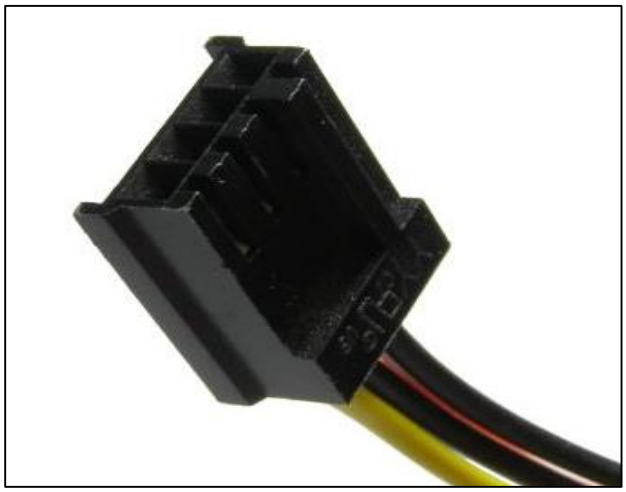

Figure 2-3 Berg connector (Female part)

The aluminum layer over the contacts needs to be removed to solder the copper wires to it. The serpentine profile is first placed on a glass slide and then covered using aluminum foil which is taped on the sides using a scotch tape. The aluminum layer is further polished with ALLIED 0.5 µm polycrystalline diamond suspension- water based paste till the copper contacts starts appearing. The specimen is further soldered to copper wires taking care that the lead from the flux does not contaminate the thin film. Soldering is undesirable due to many reasons. Firstly the flux introduces some

contamination to thin films, secondly it dissolves enough copper due to high temperature and reduces the wire cross section in the termination area and finally it sets up an undesirable electrochemical couple [34]. To avoid contamination due to soldering, copper wires were then bonded using diamond epoxy and cured in an oven at 100˚C for 5 minutes. The use of diamond paste also avoids the removal of aluminum layer from thin films and hence further avoids any entry of contamination. Figure 2-4 and Figure 2-5 shows the specimen prepared from the above procedure.

The specimen is now placed in an over inside the desiccator with dry Nitrogen gas flowing, pre-set at room temperature. The thin films are now annealed at 100˚C and then is allowed cooled slowly to room temperature. Annealing is the heating of the material above the crystallization temperature and thereafter cooling it to room temperature. It induces ductility, softens the material, relieves internal stresses, refines the structure by making it homogeneous and improves the cold working properties. Resistance measured at this point is marked as the initial resistance of the specimen. The specimen is then de-greased ALLIED® 1 µm polycrystalline diamond suspension-water based paste, IPA, deionized water and dried with dry nitrogen gas. Note the increase in resistance at this stage due to the cleaning of the specimen due to loss of metal thickness (approx. a few nm).

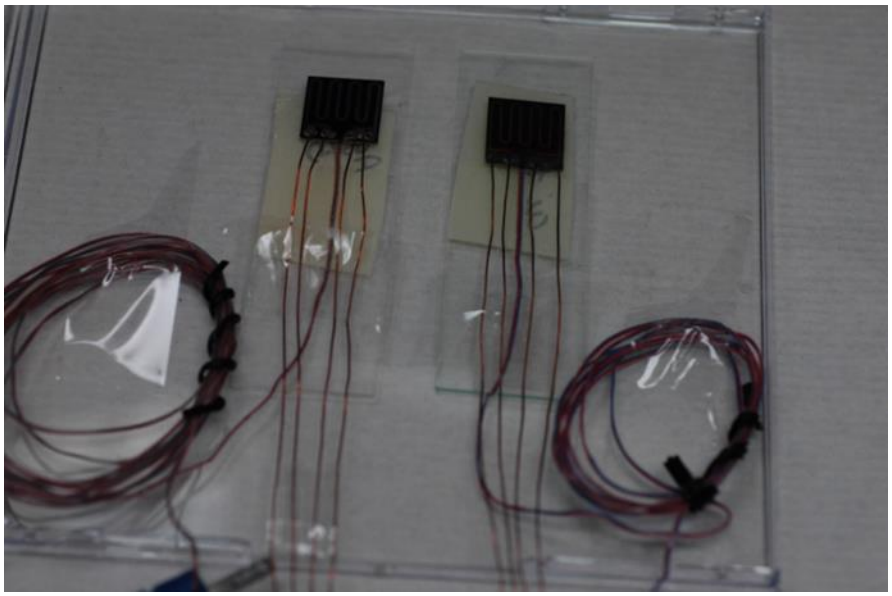

Figure 2-4 Copper and Silver thin film specimen

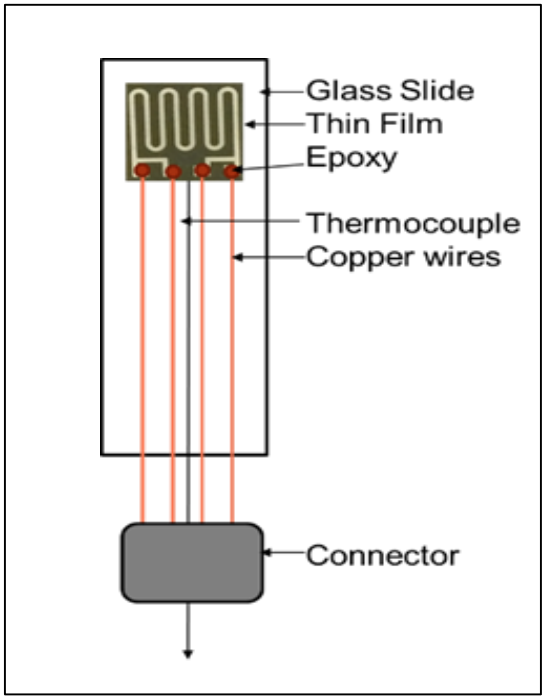

Figure 2-5 Schematics of thin film specimen

Chapter 3

Corrosion Rate Measurement

Once the copper and silver specimen is ready, similar samples are prepared for each pair of copper-silver metals for further experiments.

3.1 The Thermal Coefficient of Resistance

A temperature coefficient is the relative change of a physical property that is associated with a given change in temperature, the temperature coefficient α is defined by,

$$\frac{\Delta R}{R} = \alpha \Delta T$$

The thermal coefficient of resistance 'α' is calculated for the thin film by varying the temperature of the oven and corresponding measuring the voltage and resistance of the thin film due to the change in temperature. The thin film is placed inside the oven and the resistance at the room temperature is noted. Thereafter, the oven is heated gradually at different temperatures which would heat up the thin film and its corresponding resistance is measured. Hence temperature coefficient of resistivity (α) is calculated from the following equation,

$$R_T = R_o [1 + \alpha(T - T_o)],$$

where, R_T and R_o are the values of the resistance at temperature T and T_o, respectively. T_o is taken at room temperature. 'α' is the temperature coefficient of resistivity. Based on the above formula, α for the copper and silver thin film is value is supplied to vary the temperature of the thin film is FoS. calculated. From the value of α, the current requirement for the copper and silver thin film is calculated before placing it in the Flowers of Sulfur (FoS) chamber. Figure 3-1 shows the schematics of the thin film when placed inside the oven or environmental chamber.

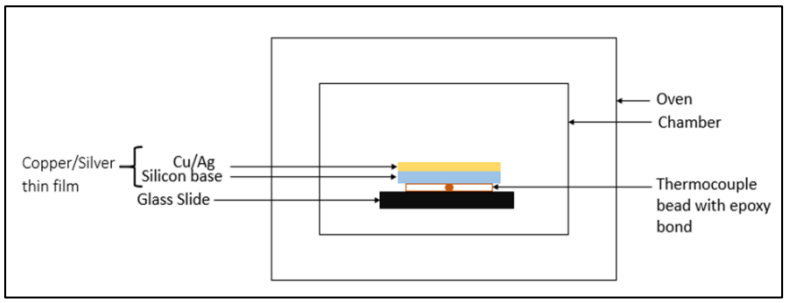

Figure 3-1 Schematics of the thin film when placed inside the environmental chamber

3.2 Environmental Test Chamber

To maintain a constant temperature throughout the experiment, the environmental chamber commonly known as oven is used. The environmental chamber has a feedback system that if the temperature inside rises beyond the set value, it stops heating. A constant value of temperature can be maintained easily and uniformly inside the chamber. This is to ensure that the sulfur will not sublimate due to non-uniform heating. The oven that was used for the experiment was not exposed to sulfur earlier. Hence it can be assured that there was no sulfur deposition on the walls of the oven. The size of the oven should be sufficient enough to accommodate the paddle wheel set-up. The oven used in this experiment was 2 feet X 2 feet X 2 feet. The oven also has a small circular opening on the top to hose the wires. Figure 3-2 shows the environmental chamber used for the experiment.

Figure 3-2 Environmental Test Chamber

3.3 Paddle Wheel set-up or The Flowers of Sulfur Chamber

Extensive research is being done in the field of corrosion to develop a test setup which can be used for testing the rate of corrosion on IT equipment. One of them is a Paddle wheel Test setup (also called as Flowers of Sulfur Chamber). A Paddle wheel or the Flowers of Sulfur Chamber is a test setup used to measure the rate of contamination in PCBs ensuring uniform air-flow distribution across it, without disturbing the operating machinery of any data center. It is an accelerated test setup of studying the effects of sulfur [11].

Paddle wheel (shown in Figure 3-3) is 1 foot x1 foot x1 foot structure. The front side of the Paddle Wheel Test Setup's has a door. The entire setup is made of acrylic and maintained air-tight using metallic frame. There is one opening which is facilitated for the motor wiring as seen in Figure 3-4 [11].

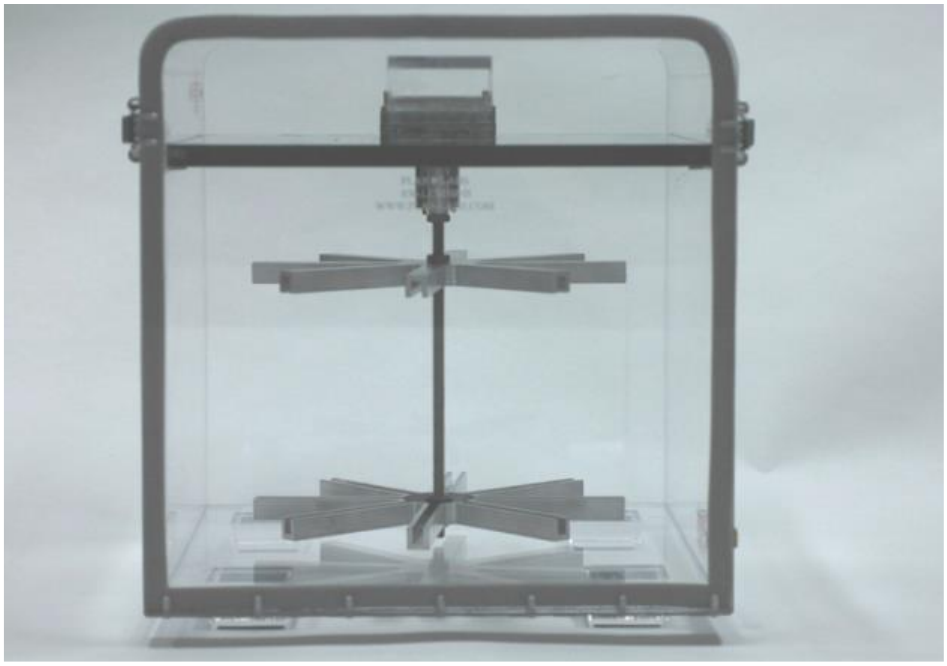

Figure 3-3 Paddle wheel Test set-up

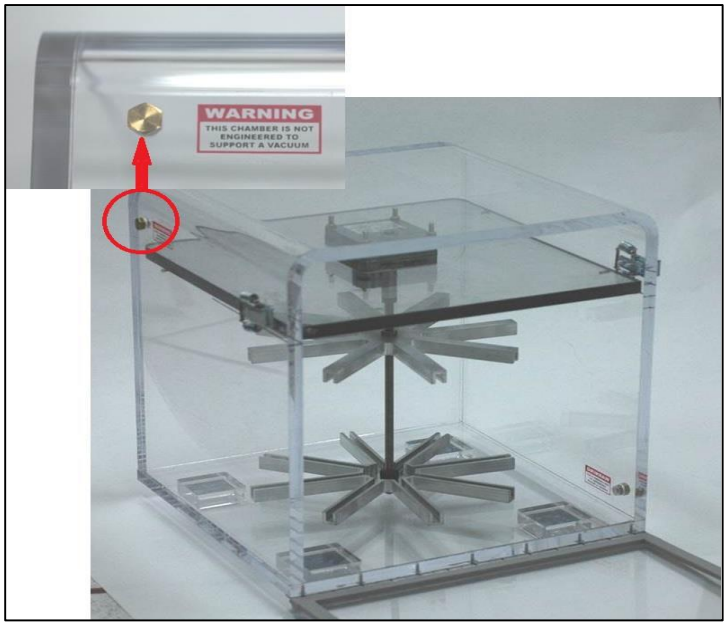

Figure 3-4 Opening for Motor Wiring

(Image source: [35])

The gear train works on a DC gear-motor. The motor has a maximum speed of 50 RPM. The shaft of the motor is connected to the central shaft through a coupling mechanism. The central shaft is runs from the coupling to the end (it does not touch the bottom). The central shaft is a solid shaft made out of steel. Its diameter is 1 centimeter and the length of the shaft is 9 inches [12].

Two aluminum carousels are mounted on the central shaft. Thus the rotary motion of the motor is transferred from the shaft to the carousels. The carousels are machined to fit test specimen into them. The diameter of the carousel is 8 inches as seen in Figure 3-5. A total of eight test specimen can be mounted between the carousels. In the actual test four copper and four silver foils were mounted on alternate carousels. These foils were used as elemental representation of the copper and silver on the Printed Circuit Boards [12].

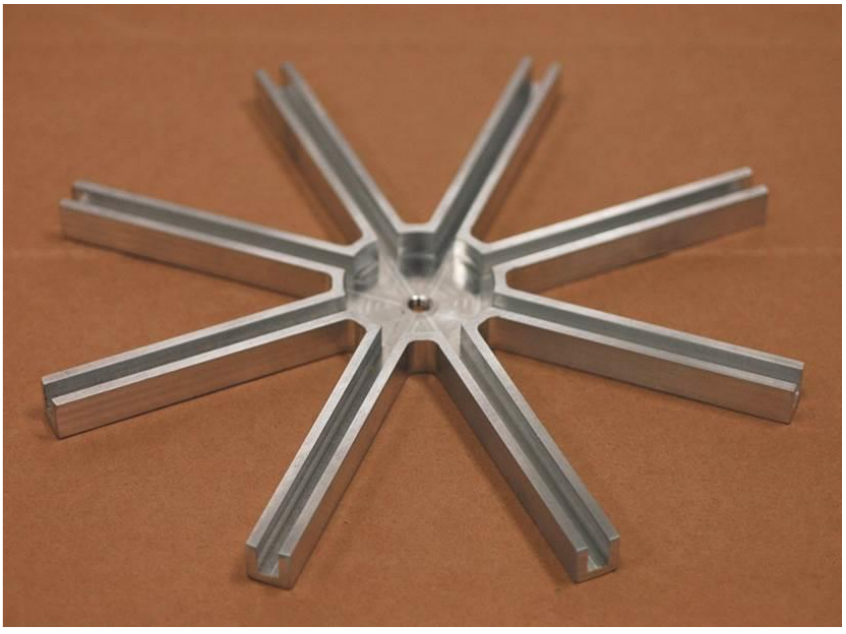

Figure 3-5 Carousel

The experiment used the sulfur powder in elemental form (S_8). The sulfur powder is placed below the carousels inside the test set-up. Two petri dishes containing saturated salt solution were also kept along with the S_8 dishes. The whole set-up is placed is then kept in an environmental test chamber to maintain the temperatures of the test set at 30˚C. As the motor was switched on the S8 in the petri dishes is displaced due to the motion of the foils placed between the carousels. This S_8 diffuses in the air in the test setup. With the increase in time the foils start absorbing the S_8. Thus, layers of reaction products are formed on the foils. The after products of the reaction were found out to be Copper Sulfide (Cu_2S) in this case from the coulometric reduction tests.

3.4 Relative Humidity

The humidity in the FoS chamber is maintained at various levels by using saturated salt solutions and the thin film temperature is maintained at various levels between 30˚C and 50˚C by the joule heating of the films. Two petri dishes containing saturated salt solutions is used to introduce relative humidity in the test setup. The petri dishes are first cleaned with deionized water and placed in aluminum foils to avoid any contamination. Then salt solution is added to the petri-dishes. It is mixed thoroughly using a stirrer and more salt solution is added until it gets saturated and doesn't dissolve any more of salt in it.

Different salt solutions give different levels of relative humidity at different temperatures. The detailed information can be obtained from Table 3-1.

Table 3-1 Relative humidity at different temperatures

Salt	Temperature (C)						
	20	25	30	35	40	50	60
	%RH						
Potassium nitrate	93	92	91	89	88	85	82
Potassium chloride	86	85	84	83	82	81	80
Ammonuim sulfate	81	80	80	80	79	79	78
Sodium chloride	76	75	75	75	75	75	75
Ammonium nitrate	65	62	59	55	53	47	42
Magnesium nitrate	55	53	52	50	49	46	43
Magnesium chloride	33	33	33	32	32	31	30

The experiment is maintained at 30˚C and hence the relative humidity at 30˚C is of our interest. Relative humidity sensors are placed right in front of the petri-dishes containing saturated salt solutions, inside the paddle wheel test set-up to monitor the value.

3.5 Gaseous Contaminant

The gaseous contamination is provided in the form of free sulfur powder. The amount of sulfur to be considered is based on the chart provided by Battelle as shown inFigure 3-6. Based on the graph, approximately 70 ppb free sulfur needs to be considered at 30°C. The free sulfur is placed in a dish and is kept below the paddle wheel in the chamber. The oven is set to 30°C and the sulfur is baked for an hour to ensure that it is moisture-free. Care has to be taken to avoid direct contact of sulfur with eyes and skin as it can be harmful and can produce irritation. The main challenge in using sulfur is to maintain a constant temperature within the chamber as the sulfur would sublimate. Figure 3-7 shows the set-up once the sulfur and saturated salt solutions are placed inside the FoS chamber.

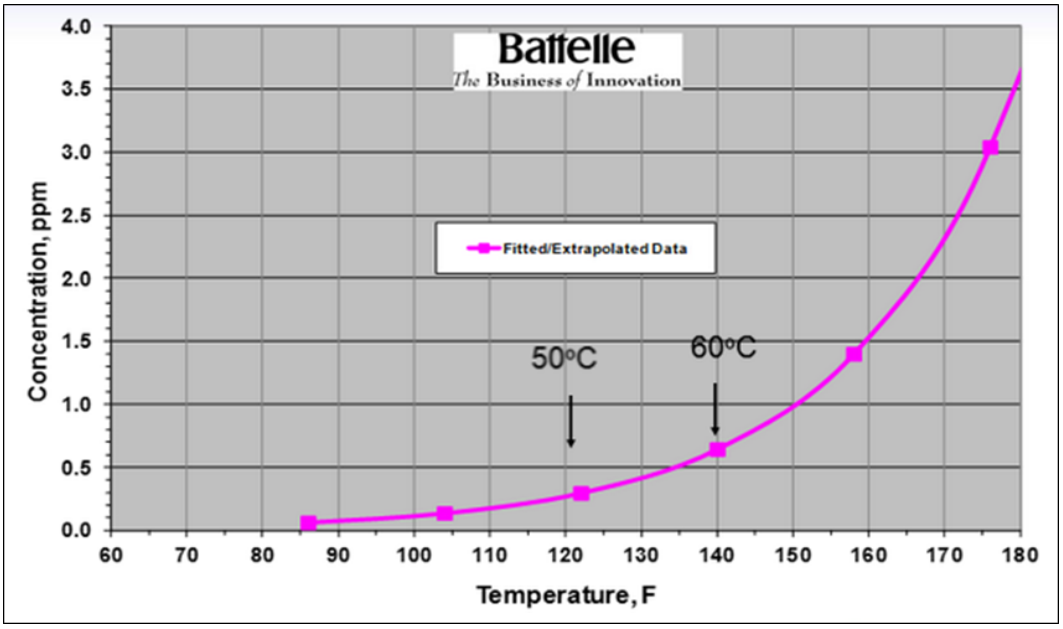

Figure 3-6 Concentration of sulfur vapor (S8) by volume vs. Temperature

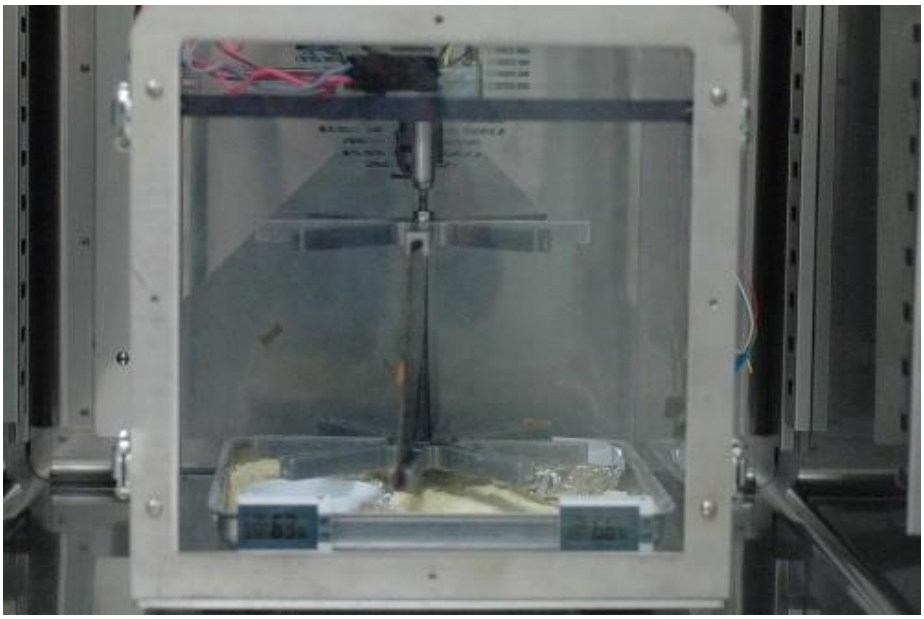

Figure 3-7 Flowers of Sulfur chamber with paddle wheel test set-up along with sulfur and saturated salt solutions

The corrosion rates of copper and silver, in a 30^{o}C ambient with ~70 ppb free sulfur, are plotted in the upper right corner of the ASHRAE A1-A4 allowable temperature-humidity ranges.

3.6 Corrosion Coupons

The use of copper–silver coupons as a reactive monitoring technique has been used widely to find the amount of corrosion occurring in datacenters. The purity of these coupons is 99.9%. Rectangular strips with area of 1935.5 mm^2 are cut. Sand paper of very fine grain size is used to rub against the smooth side of the film using acetone. This process will ensure that there are no particulate and gaseous contaminants present over the surface of the thin film. It is further cleaned with acetone, deionized water and dried

with dry Nitrogen gas. Once the samples are ready, the copper- silver coupons are placed on two opposite sides in a small plastic box using a sticker tape. These boxes are then placed in a chamber with dry nitrogen gas flowing through it.

Chapter 4

Experiment

Once the specimen is prepared and annealed, the experiment follows the following procedure.

1. The initial resistance of the copper silver thin film is calculated by supplying a 5mA of current. Small amount of current will not lead to any joules heating and the voltage across it is measured. The thickness corresponding to the resistance is the initial thickness, i.e t_1.
2. The thermal coefficient of resistance for thin films is now calculated by heating the environmental chamber at various temperatures and measuring the corresponding temperature of the thin films. The temperature is measured using a digital thermometer (Z190A) shown inFigure 4-1. The wires from the male berg connector is connected with the female connector which is eventually connected with the power source to supply different levels of current. The thermocouple is connected with the FLUKE® Selector Thermocouple to read the temperature readings with its corresponding wire codes as shown in Figure 4-2.

Figure 4-1 Digital Thermometer (Z190A)

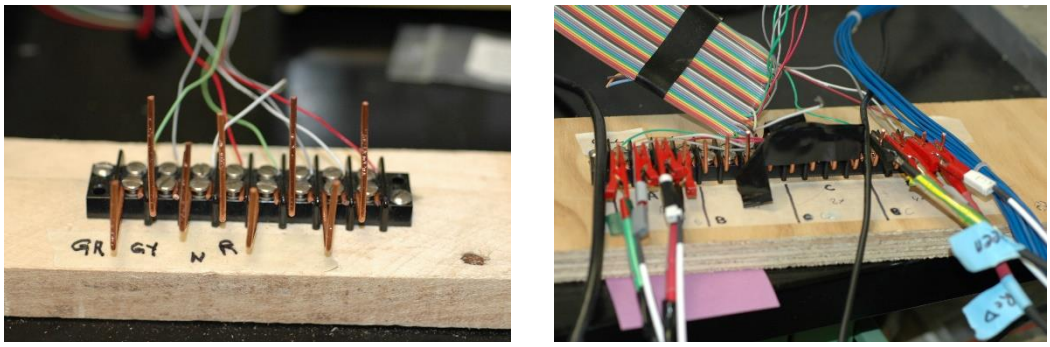

(a) (b)

Figure 4-2 Connections to the digital thermometer (a) without wiring and (b) with wiring

Once the value of thermal coefficient of resistance is calculated, the power requirements, i.e. the current required to attain different levels of thin film temperature is to be found out using hit and trial method.

3. The environmental chamber is pre-set to 30° C and the sulfur is allowed to baked for half an hour. Saturated salt solutions is prepared and is placed inside the paddle wheel test set-up and the motor is turned on for uniform distribution of air within the chamber.
4. The thin films are cleaned at this point before placing it inside the chamber for the corrosion test. It is de-greased with ALLIED® 1 µm polycrystalline diamond suspension-water based paste, IPA, deionized water and dried with dry nitrogen gas. Note the change in resistance and its corresponding thickness.
5. The cleaned specimen is now placed on the spare front door of the paddle wheel chamber or the FoS chamber. Provisions has been made by using a wooden ply to position the thin film specimen. Copper and silver coupons are also taped on

the lateral sides of the thin film. This ensures that the specimen and coupons are at same height.

6. The oven is opened and the existing front door of the FoS chamber is replaced with the spare door and is latched quickly so that the set-up is not disturbed.
7. One additional thermocouple is also placed inside the FoS chamber to monitor the temperature within the chamber.
8. Different values of current that are to be applied are stored as an input to VersaSTAT software ® and which initiates the experiment.
9. The temperature values can be updated at different intervals on the FLUKE® Selector Thermocouple instrument. In this experiment, the temperature was measured at every 10 minutes.
10. The voltage across the resistance is updated by the VersaSTAT software.
11. Relative humidity is monitored manually every 2 hours during the experiment.
12. After the experiment is completed, the thin film and coupons are stored in a CD drive box in a cool and dry place. Details like specimen number, relative humidity value, run time for the experiment, etc is mentioned on the CD cover for future reference.
13. The values of current, voltage and temperature of the chamber and thin film is plotted on excel sheet. Resistance of the thin film is calculated and this is the uncompensated resistance. The uncompensated resistance is the resistance of the pure metal and the corroded metal. The uncompensated resistance is calculated using the equation of thermal coefficient of resistance. The values of α calculated for each case would be used in this calculation.

14. From the uncompensated resistance, the remaining thickness of pure metal is found and based on the amount of metal that is corroded, the corrosion rate is calculated.
15. The corrosion rate is calculated by subtracting the difference of two consecutive thickness over a constant period of time.

4.1 Concept of Compensated Resistance

Let us consider a thin film with known thickness t_o and resistance R_o at room temperature T_o. The film is installed in a flowers of sulfur chamber maintained at temperature T. The film corrodes in the flowers of sulfur chamber. With time in the chamber, corrosion decreases the film thickness and increases its resistance. The thickness of the film t_T at any temperature T can be calculated if its resistance R_T is known at temperature T:

$$R_o = \left(\frac{\sigma_o l}{w}\right)\frac{1}{t_o}$$

$$\left(\frac{\sigma_o l}{w}\right) = R_o t_o$$

If the film with resistance R_T at temperature T is cooled to room temperature T_o, its resistance at room temperature R_{T0} can be calculated as follows. R_{T0} is the temperature compensated resistance of the film.

$$R_T = R_{T0}\left(1+\alpha\left(T-T_0\right)\right)$$

$$R_{T0} = \frac{R_T}{\left(1+\alpha\left(T-T_0\right)\right)}$$

The thickness of the corroded film will be

$$t_T = \left(\frac{\sigma_0 l}{w}\right)\frac{1}{R_{T0}} = \frac{R_0 t_0}{R_{T0}} = \frac{R_0 t_0}{\frac{R_T}{\left(1+\alpha\left(T-T_0\right)\right)}} = \frac{\left(R_0 t_0\right)}{R_T}\left(1+\alpha\left(T-T_0\right)\right)$$

In the above calculation we are neglecting the thermal expansion of the film.

Chapter 5

Results

5.1 Thin Films Corrosion Rate

5.1.1 Relative Humidity 33%

a) Thermal coefficient of resistivity of Copper (After Annealing)

From the experiment, the value of Thermal coefficient of resistivity, α for copper is 0.0037369/ ˚C against the standard value of 0.0039/ ˚C.

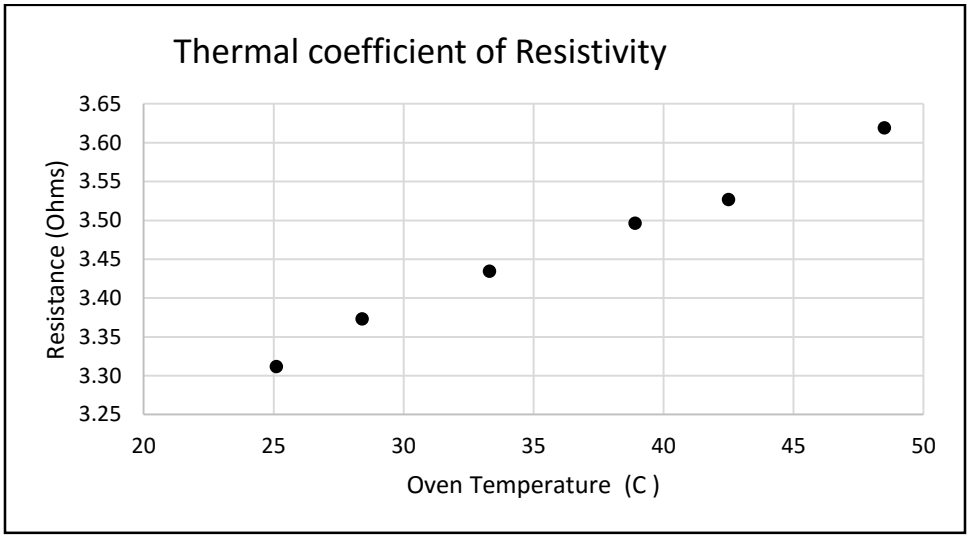

Figure 5-1 Thermal Coefficient of Resistivity for Copper

b) Thermal coefficient of resistivity of Silver (After Annealing)

From the experiment, the value of Thermal coefficient of resistivity, α for silver is 0.0028 / ˚C against the standard value of 0.004/ ˚C

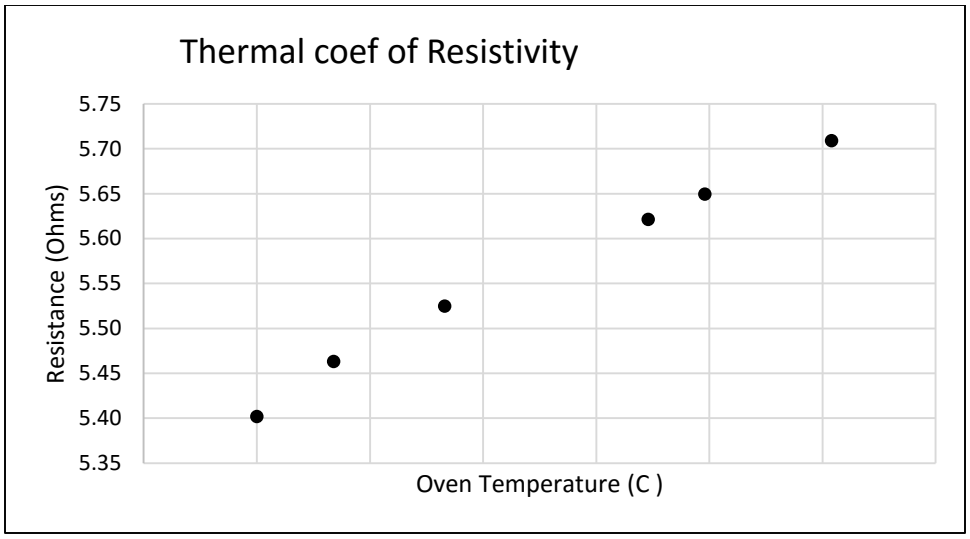

Figure 5-2 Thermal Coefficient of Resistivity for Silver

c) Copper Corrosion Rate

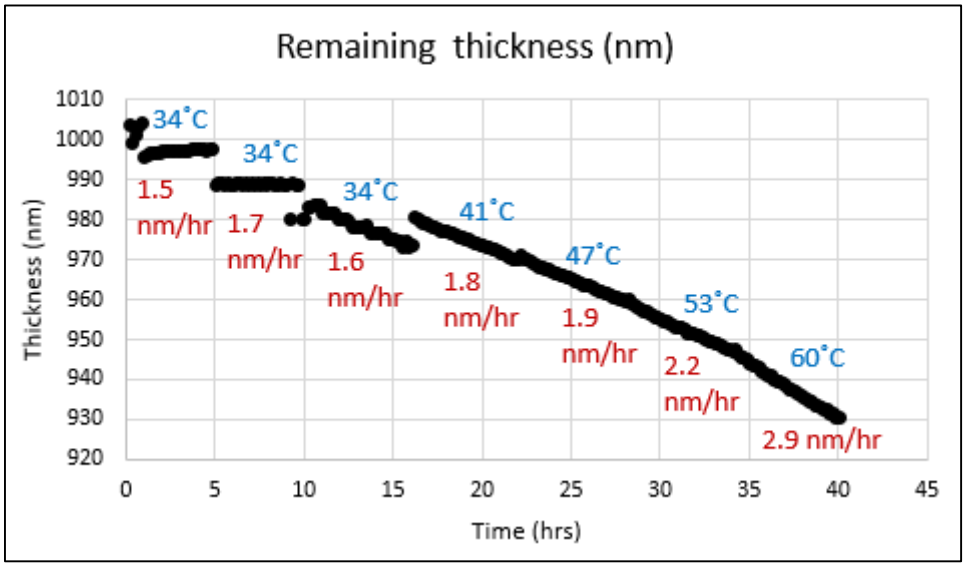

Figure 5-3 Copper Corrosion Rate

d) Silver Corrosion Rate

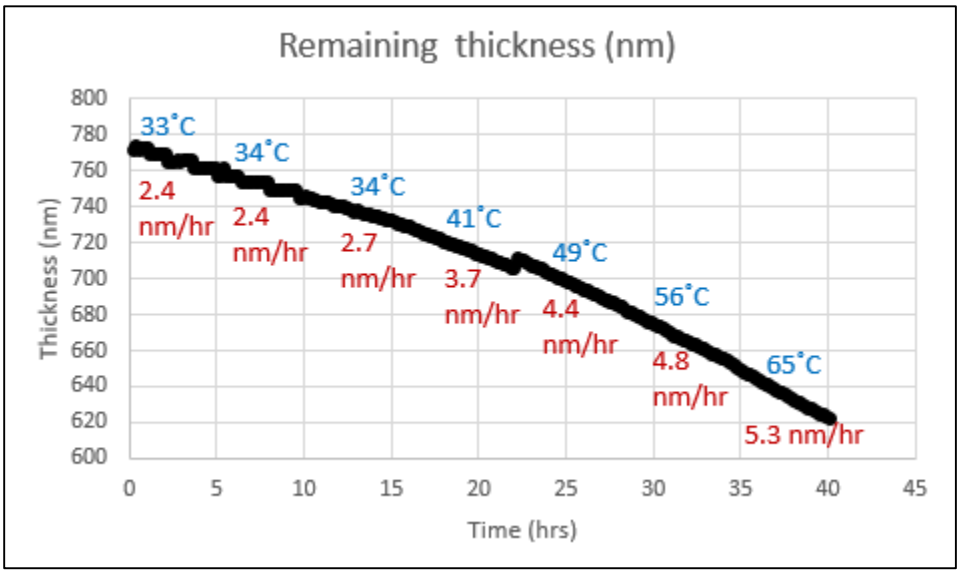

Figure 5-4 Silver Corrosion Rate

e) Combined Copper- Silver Corrosion Rate

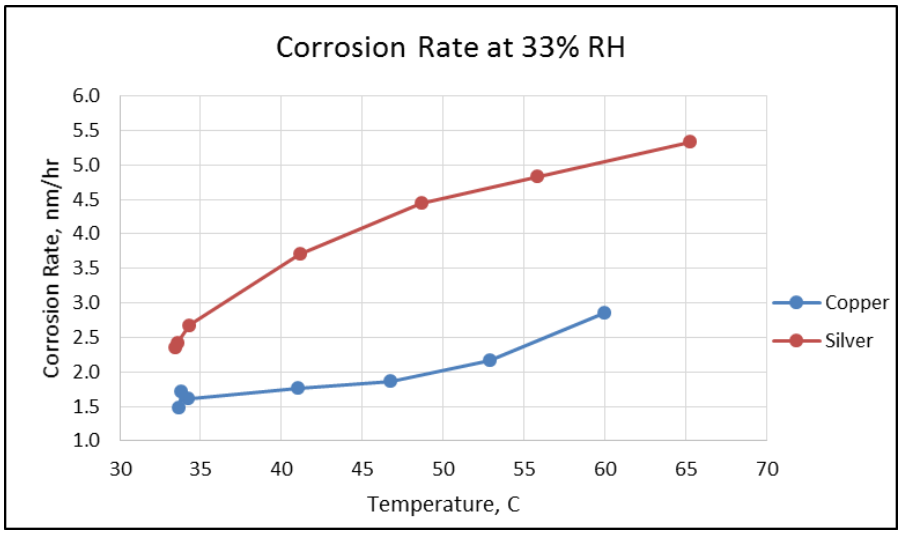

Figure 5-5 Combined Corrosion Rate for Copper and Silver

5.1.2 Relative Humidity: 52%

a) Thermal coefficient of resistivity of Copper (After Annealing)

From the experiment, the value of Thermal coefficient of resistivity, α for copper is 0.00375/ ˚C against the standard value of 0.0039/ ˚C.

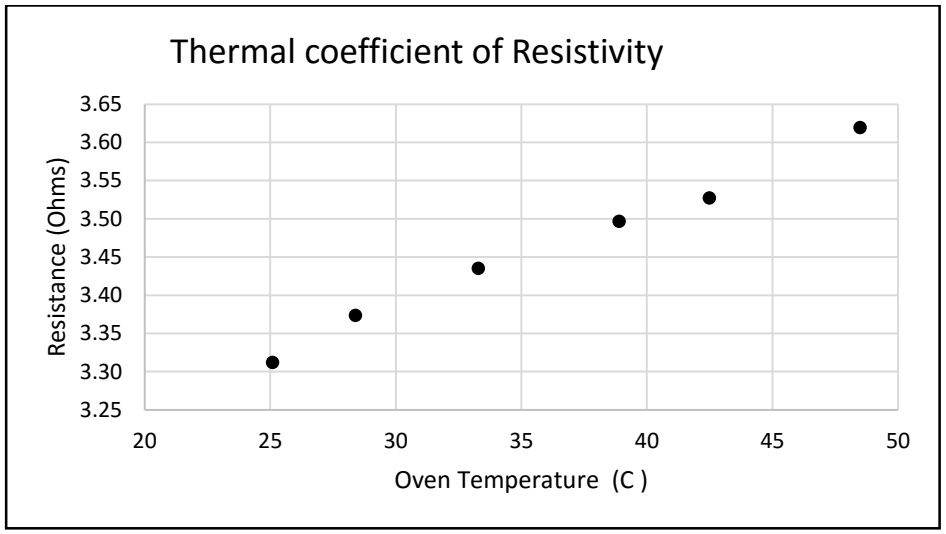

Figure 5-6 Thermal Coefficient of Resistivity for Copper

b) Thermal coefficient of resistivity of Silver (After Annealing)

From the experiment, the value of Thermal coefficient of resistivity, α for silver is 0.00304 / ˚C against the standard value of 0.004/ ˚C

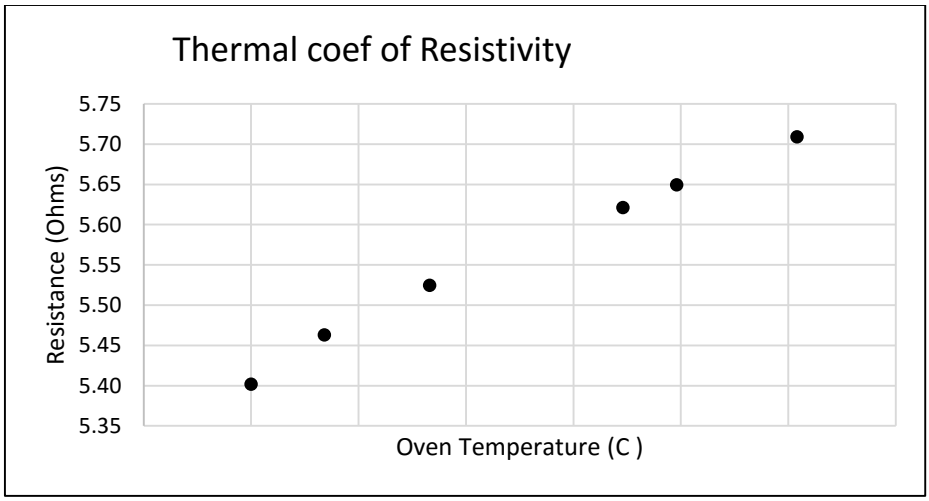

Figure 5-7 Thermal Coefficient of Resistivity for Silver

c) Copper Corrosion Rate

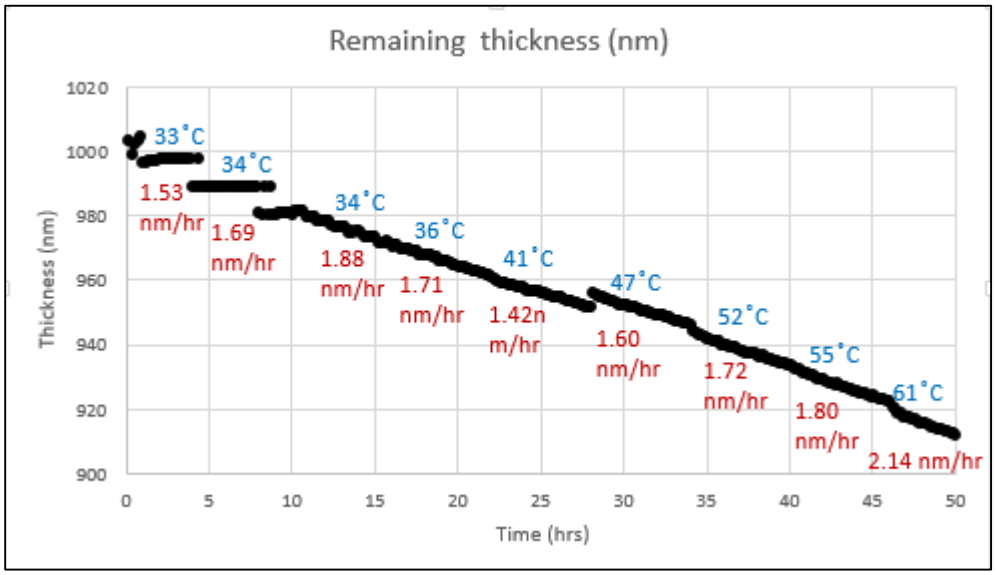

Figure 5-8 Copper Corrosion Rate

d) Silver Corrosion Rate

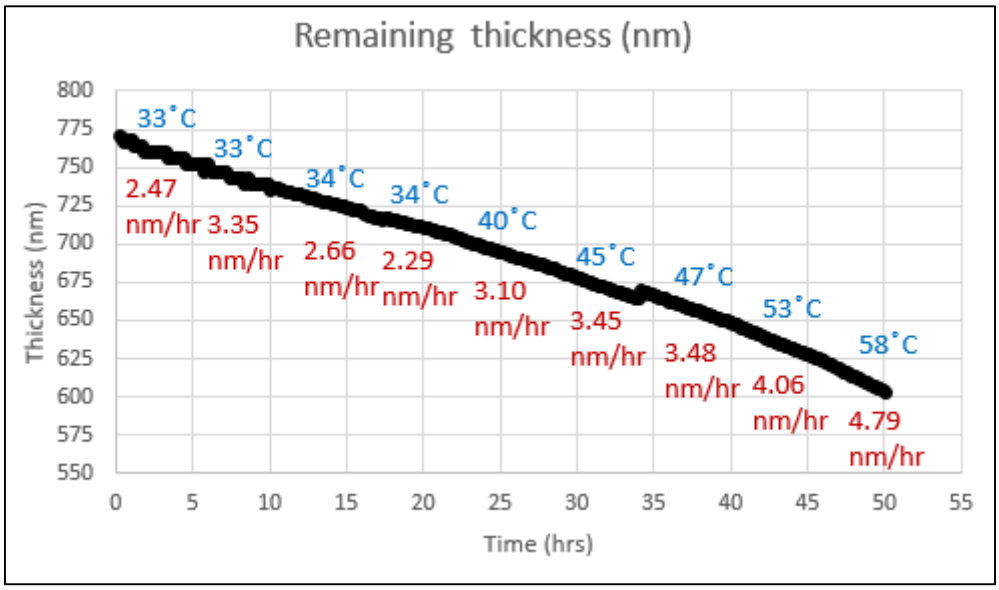

Figure 5-9 Silver Corrosion Rate

e) Combined Copper-Silver Corrosion Rate

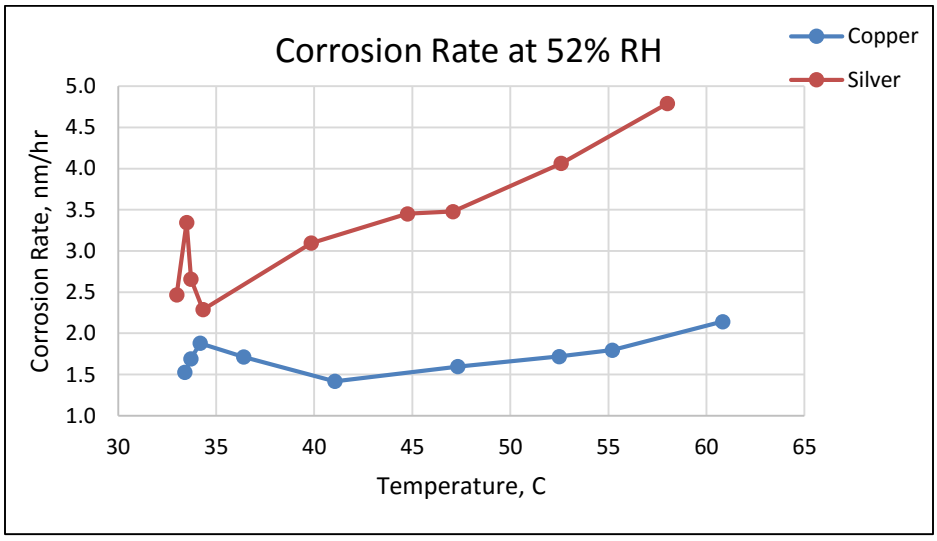

Figure 5-10 Combined Corrosion Rate for Copper and Silver

5.1.3 Relative Humidity: 59%

a. Thermal coefficient of resistivity of Copper (After Annealing)

From the experiment, the value of Thermal coefficient of resistivity, α for copper is 0.00334/ ˚C against the standard value of 0.0039/ ˚C

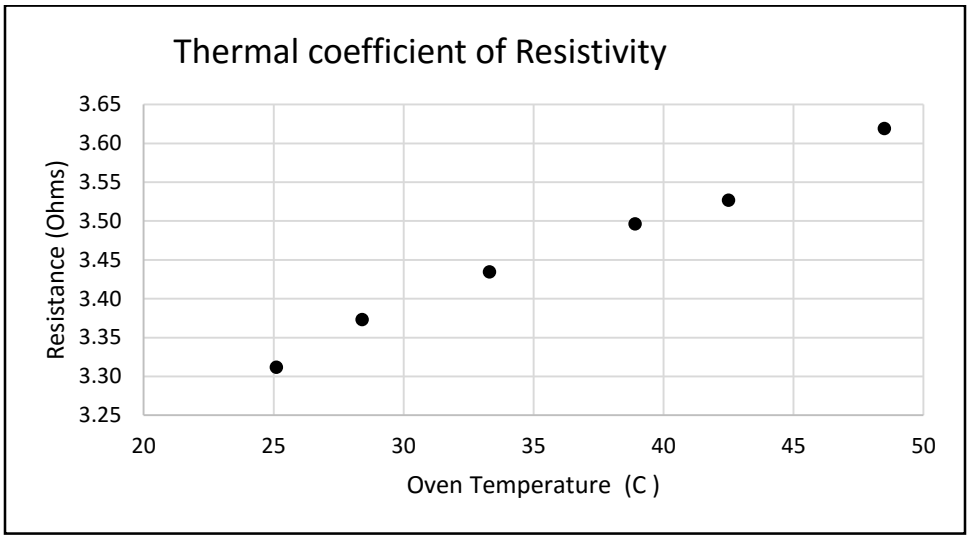

Figure 5-11 Thermal Coefficient of Resistivity for Copper

b. Thermal coefficient of resistivity of Silver (After Annealing)

From the experiment, the value of Thermal coefficient of resistivity, α for silver is 0.00305/ ˚C against the standard value of 0.0039/ ˚C

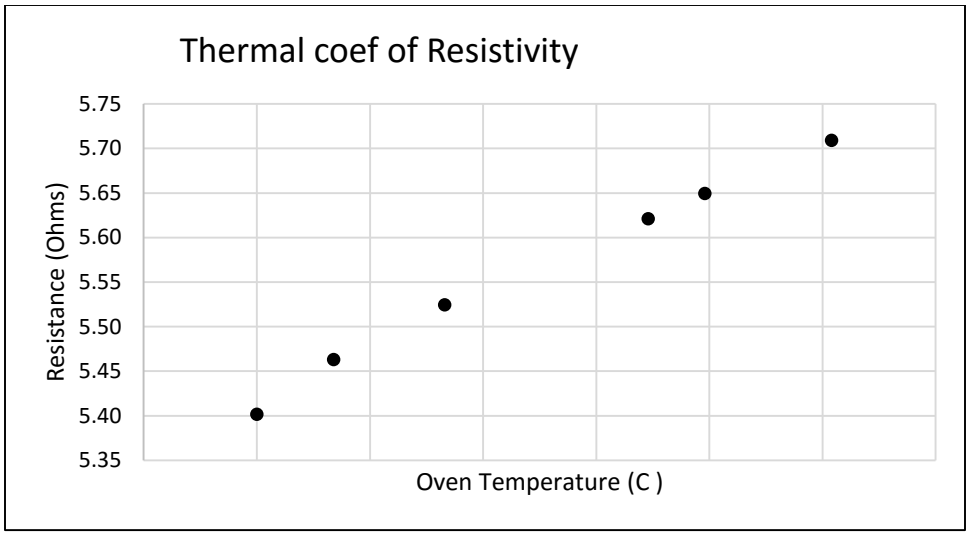

Figure 5-12 Thermal Coefficient of Resistivity for Silver

c) Copper Corrosion Rate

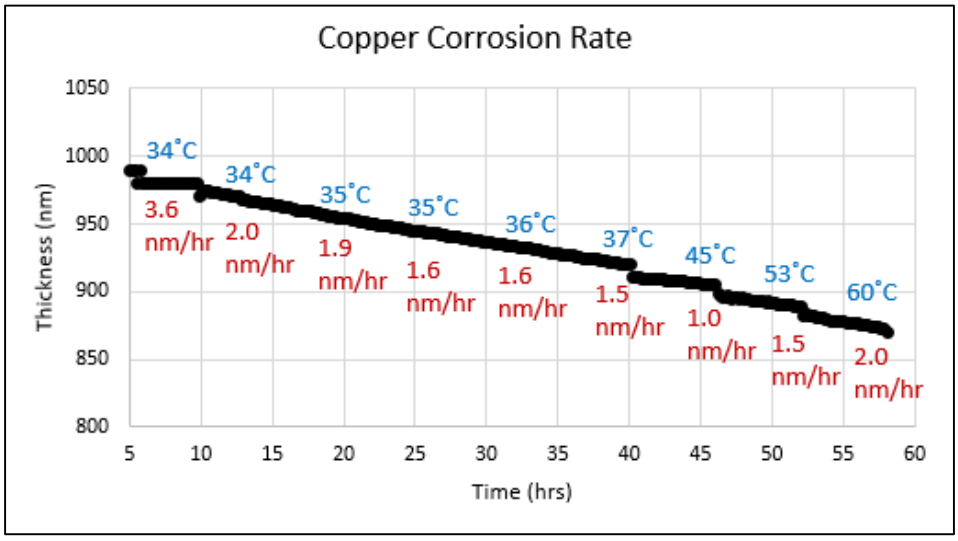

Figure 5-13 Copper Corrosion Rate

c) Silver Corrosion Rate

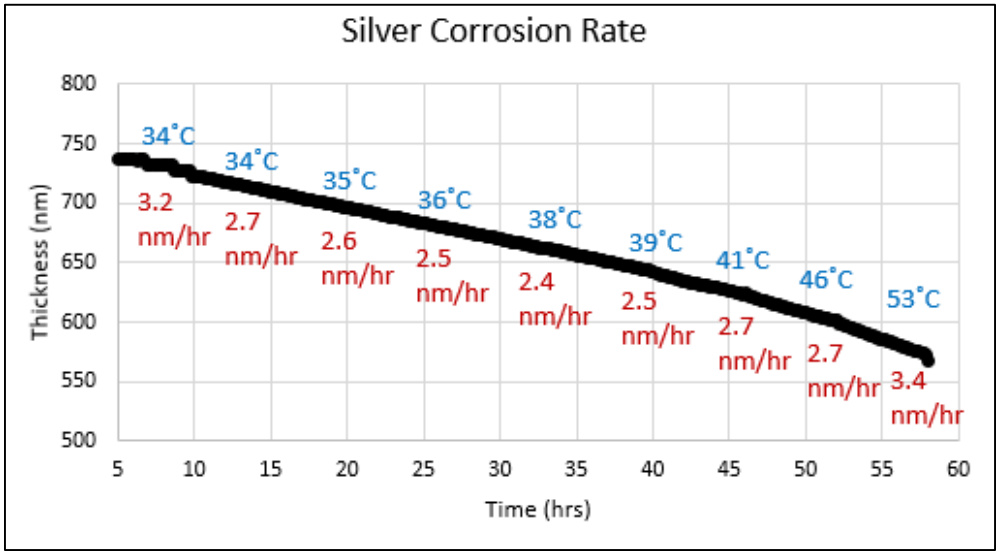

Figure 5-14 Silver Corrosion Rate

d) Combined Copper-Silver Corrosion Rate

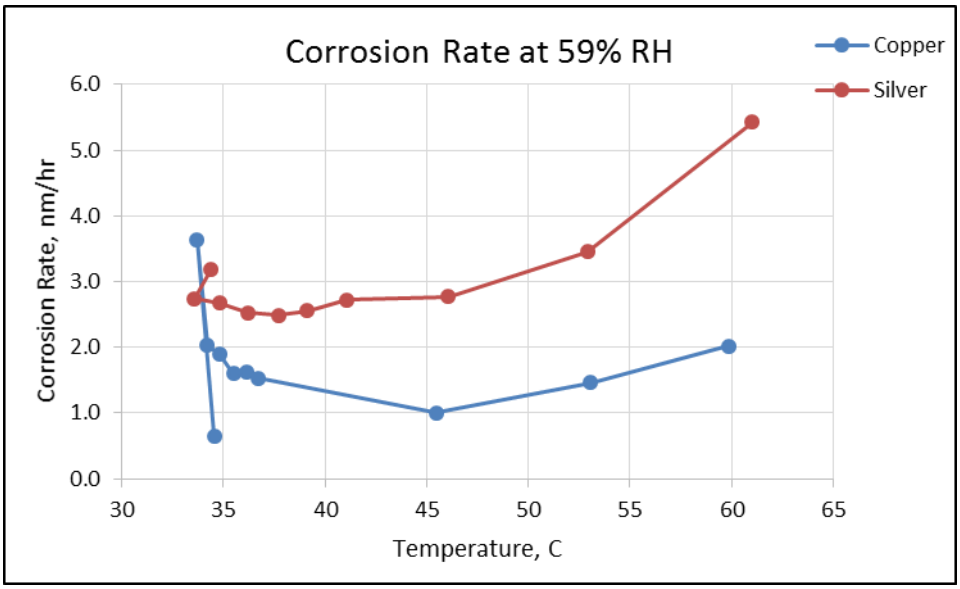

Figure 5-15 Combined Corrosion Rate for Copper and Silver

5.1.4 Relative Humidity: 75%

a) Thermal coefficient of resistivity of Copper (After Annealing)

From the experiment, the value of Thermal coefficient of resistivity, α for copper is 0.00337/ ˚C against the standard value of 0.0039/ ˚C

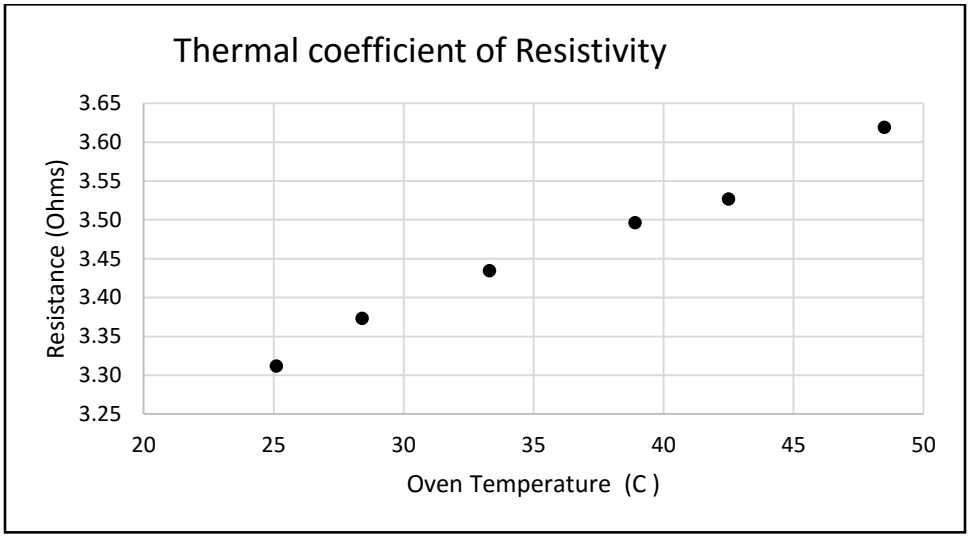

Figure 5-16 Thermal Coefficient of Resistivity for Copper

b) Thermal coefficient of resistivity of Silver (After Annealing)

From the experiment, the value of Thermal coefficient of resistivity, α for silver is 0.00327/ ˚C against the standard value of 0.0039/ ˚C

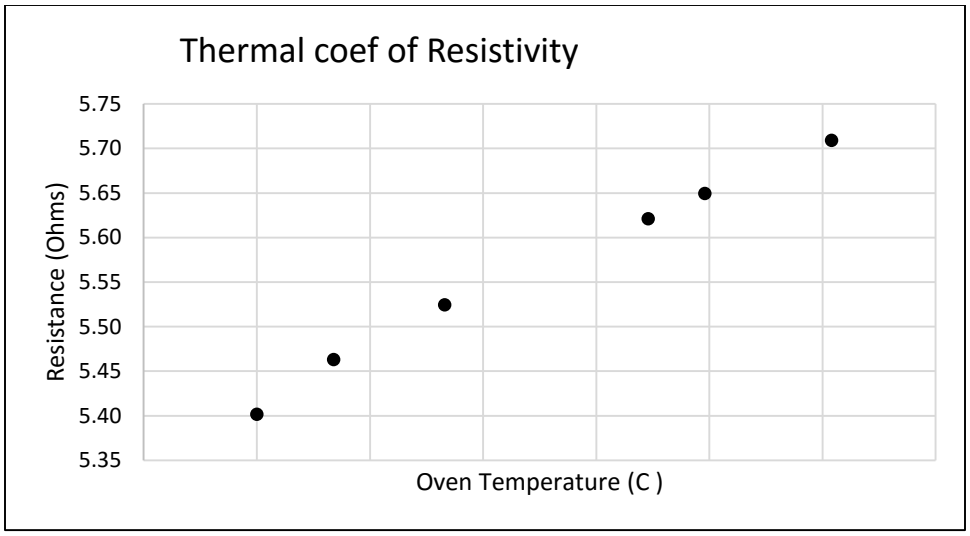

Figure 5-17 Thermal Coefficient of Resistivity for Silver

c) Copper Corrosion Rate

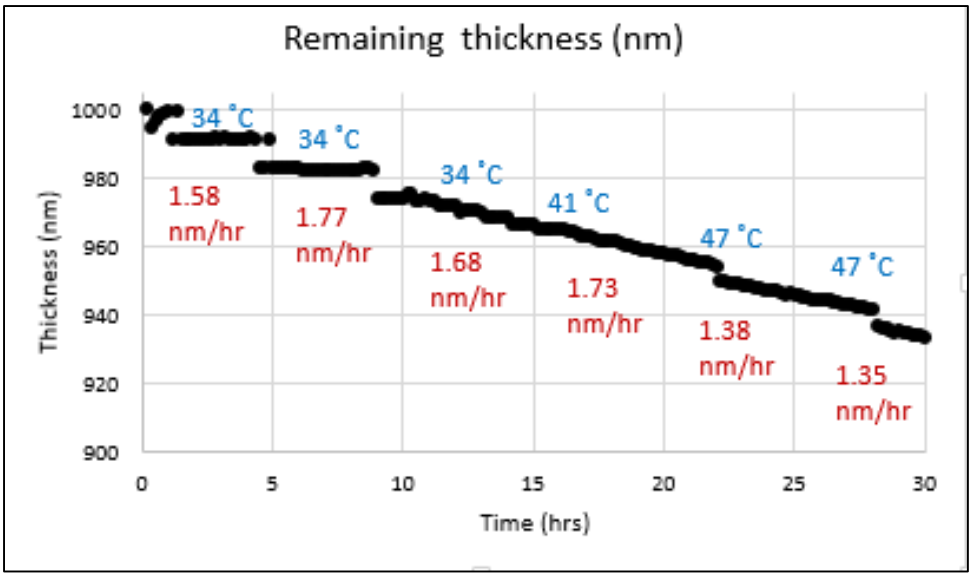

Figure 5-18 Copper Corrosion Rate

d) Silver Corrosion Rate

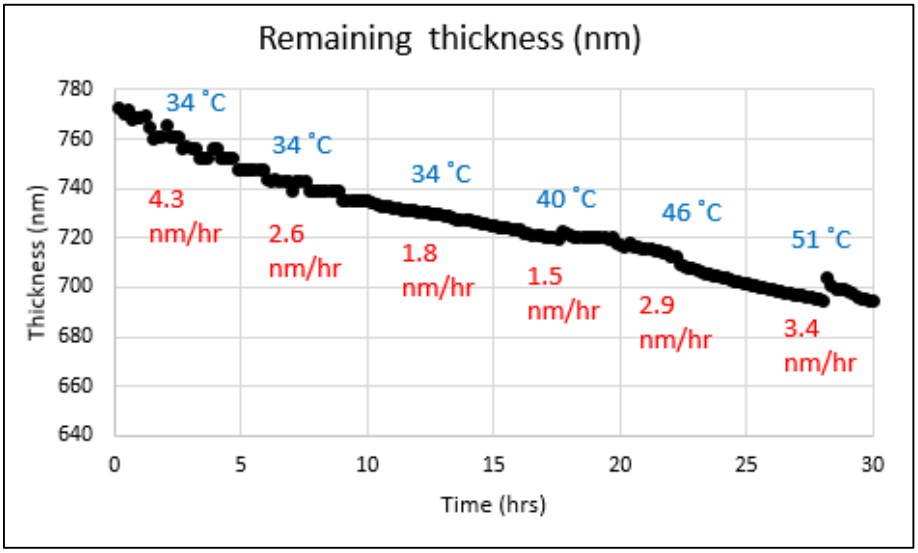

Figure 5-19 Silver Corrosion Rate

e) Combined Copper-Silver Corrosion Rate

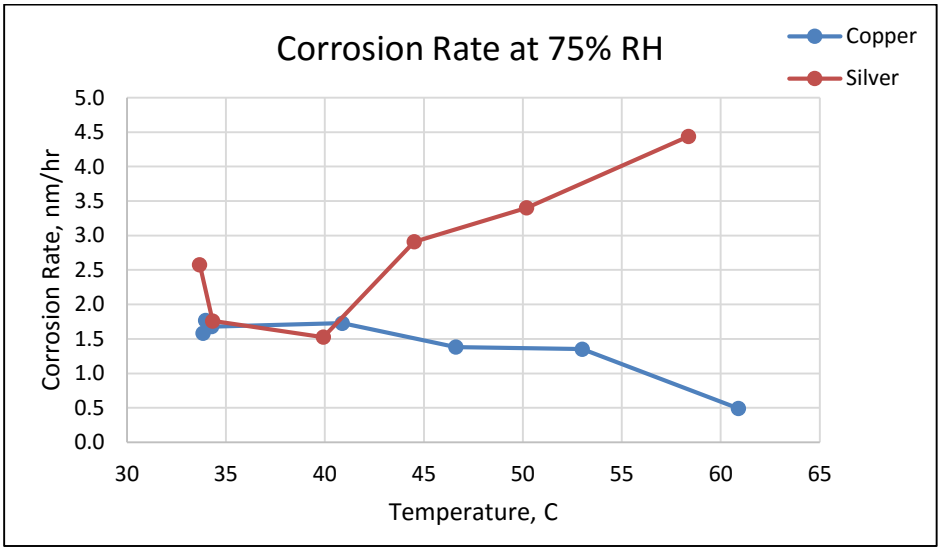

Figure 5-20 Combined Corrosion Rate for Copper and Silver

5.1.5 Relative Humidity: 84%

a) Thermal coefficient of resistivity of Copper (After Annealing)

From the experiment, the value of Thermal coefficient of resistivity, α for copper is 0.00306/ ˚C against the standard value of 0.0039/ ˚C

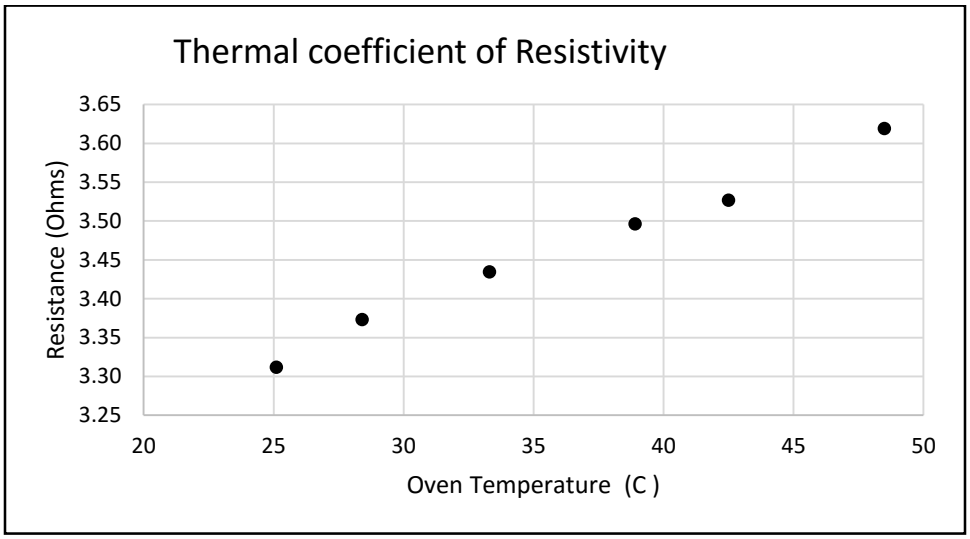

Figure 5-21 Thermal coefficient of resistivity of Copper

b) Thermal coefficient of resistivity of Silver (After Annealing)

From the experiment, the value of Thermal coefficient of resistivity, α for silver is 0.00264/ ˚C against the standard value of 0.0039/ ˚C

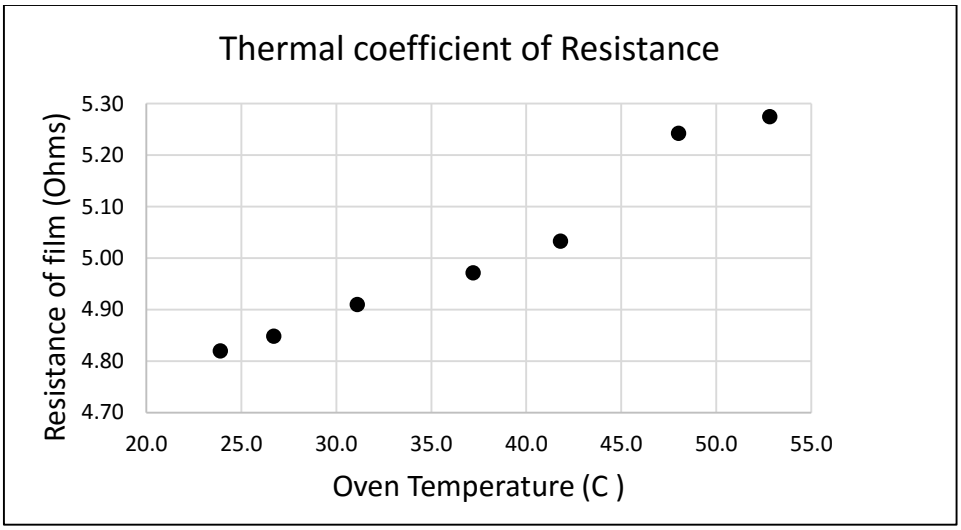

Figure 5-22 Thermal coefficient of resistivity of Silver

c) Copper Corrosion Rate

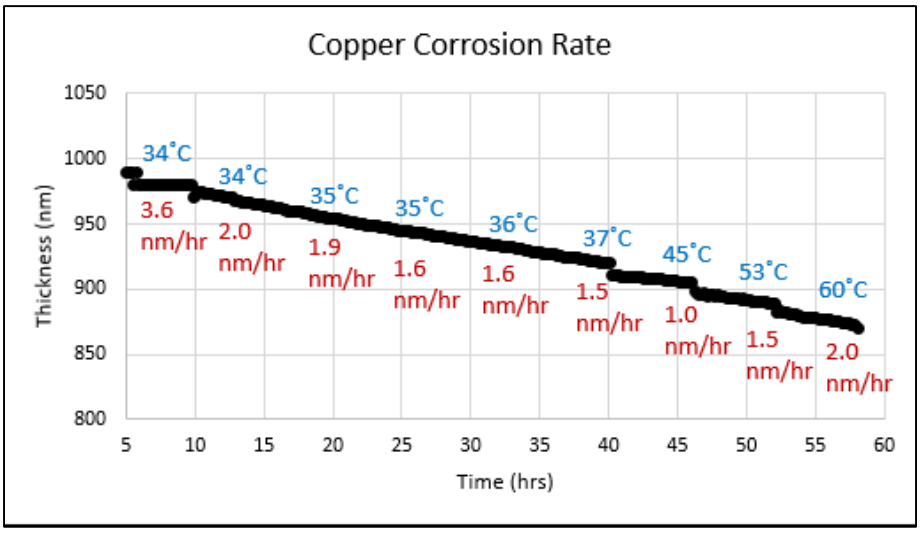

Figure 5-23 Copper Corrosion Rate

d) Silver Corrosion Rate

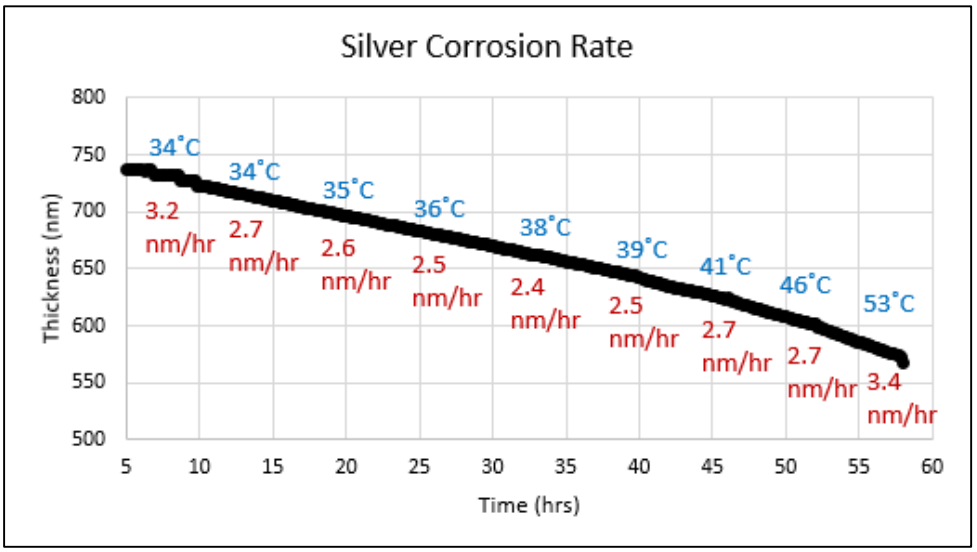

Figure 5-24 Silver Corrosion Rate

e) Combined Copper-Silver Corrosion Rate

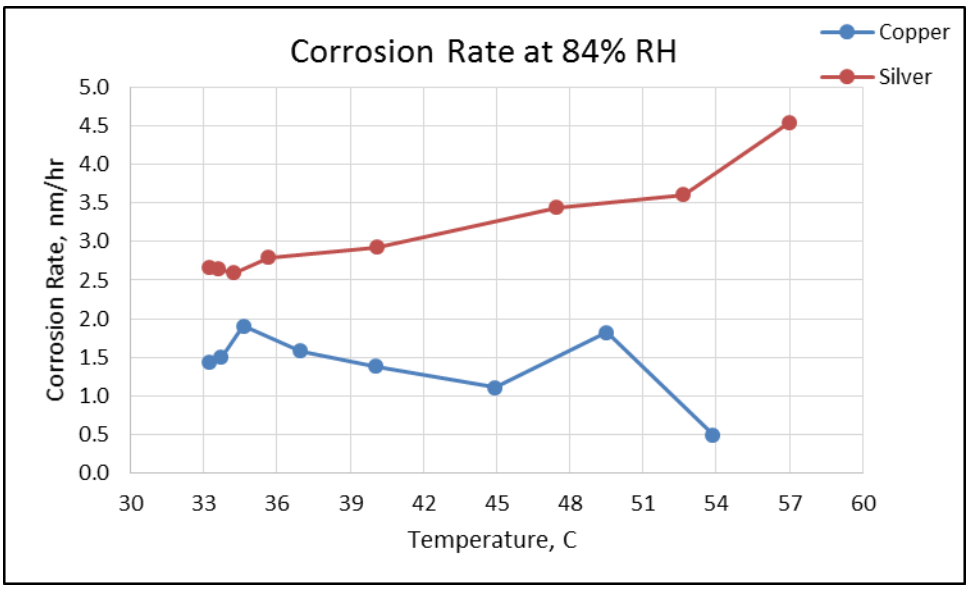

Figure 5-25 Combined Corrosion Rate for Copper and Silver

5.1.6 Relative Humidity: 91%

1. Thermal coefficient of resistivity of Copper (After Annealing)

From the experiment, the value of Thermal coefficient of resistivity, α for copper is 0.00379/ ˚C against the standard value of 0.0039/ ˚C

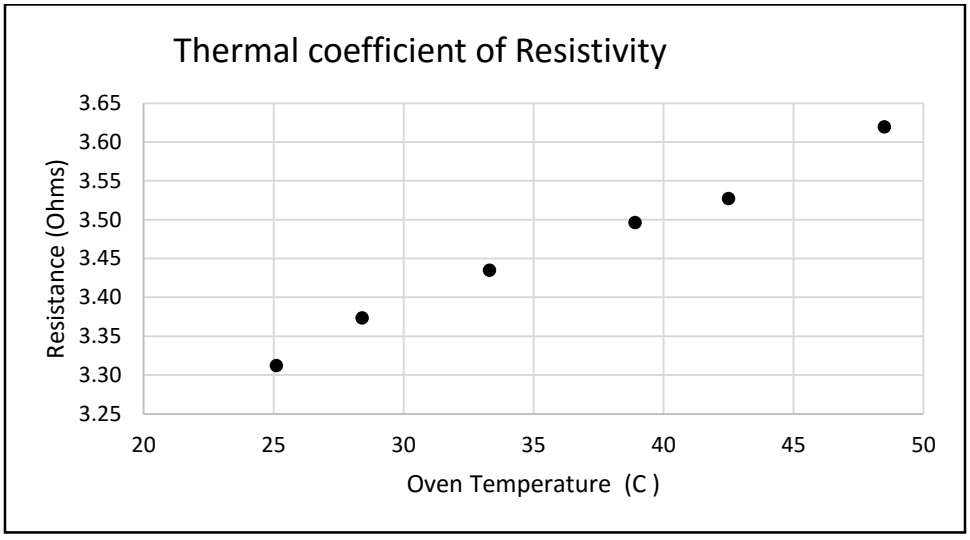

Figure 5-26 Thermal coefficient of resistivity of Copper

2. Thermal coefficient of resistivity of Silver (After Annealing)

From the experiment, the value of Thermal coefficient of resistivity, α for silver is 0.00337/ ˚C against the standard value of 0.0039/ ˚C

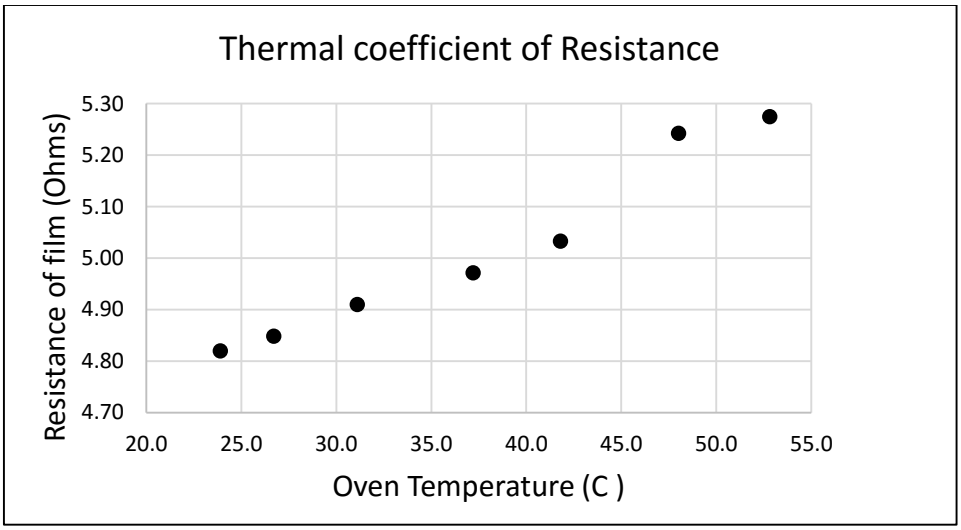

Figure 5-27 Thermal coefficient of resistivity of Silver

3. Copper Corrosion Rate

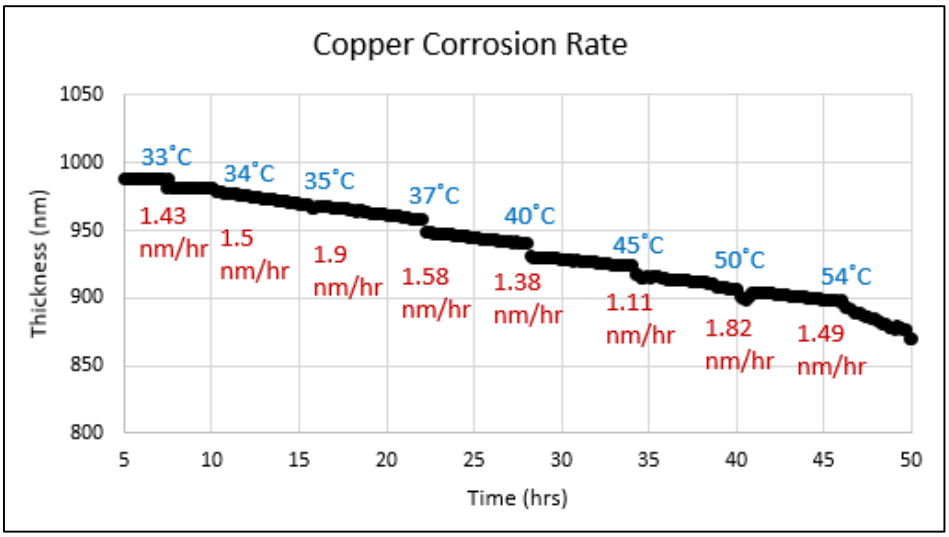

Figure 5-28 Copper Corrosion Rate

4. Silver Corrosion Rate

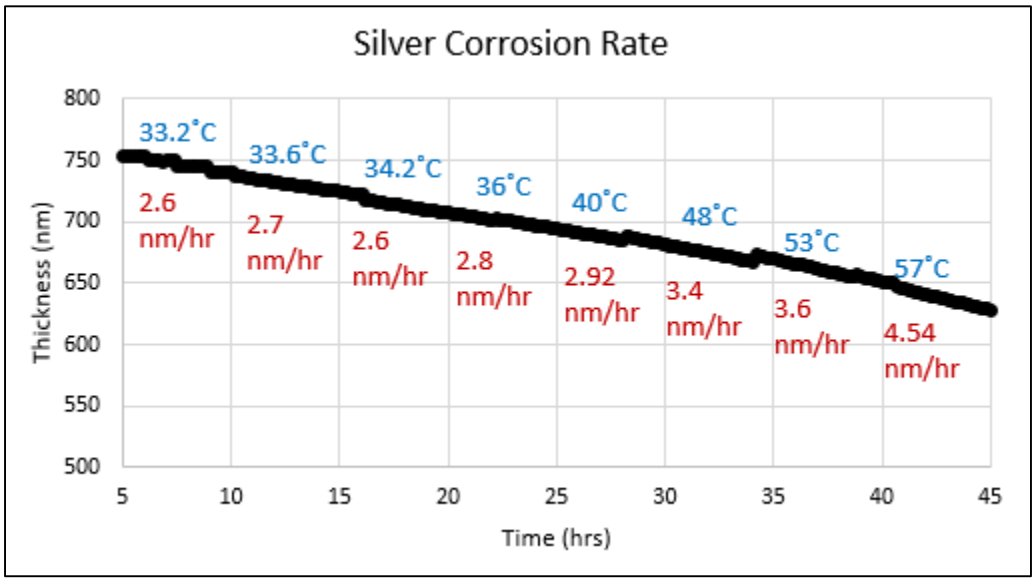

Figure 5-29 Silver Corrosion Rate

5. Combined Copper-Silver Corrosion Rate

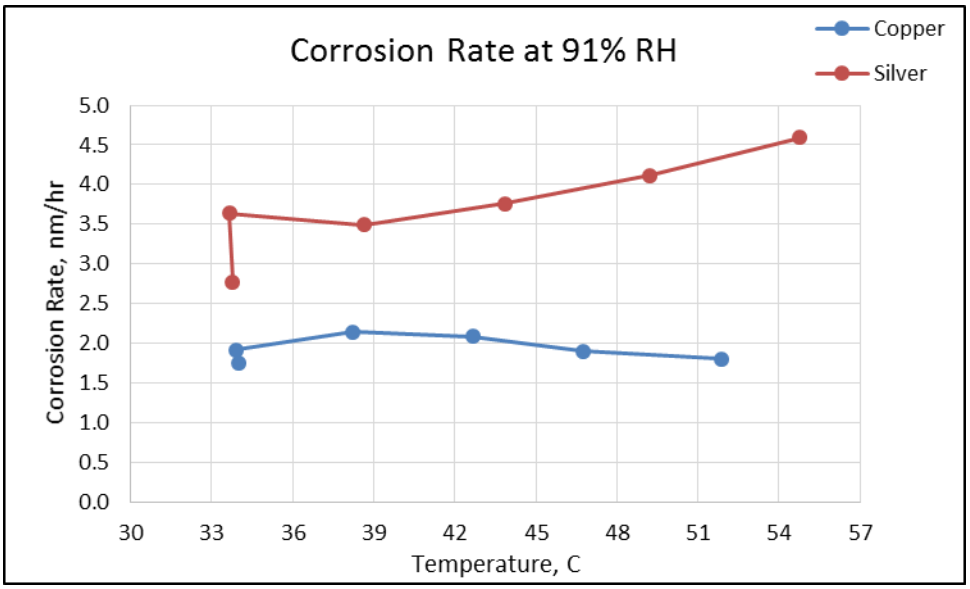

Figure 5-30 Combined Corrosion Rate for Copper and Silver

5.2 Corrosion Coupons

5.2.1 Coulometric Reduction

To determine the amount of corrosion that has occurred on the coupon, Coulometric reduction technique is used. “A Coulometric reduction or a constant-current electrolytic reduction is a standard procedure used for determining the relative build-up of corrosion and tarnish films on the control coupons from environmental tests, and discuss the types of results and correlations that may be expected” as sited by Krumbein, S. J, et al [36]. There are various techniques to determine the relative built up of corrosion such as the weight gain method, coulometric test, etc. The weight gain method is a non-destructive process and can be used only for finding out the total amount of excess mass a metal has gained due to the environmental attack. Any information related to the products of the reaction is not obtained from this method. On the other side, Coulometric reduction technique, it is possible to resolve the reaction products into its major individual chemical constituents. A detailed understanding of the results can be made eventually.

In this technique, a constant current density is applied to the sample placed in an electrolytically conductive solution which results in variation in potential, measured against the standard reference electrode in the same solution, as a function of time. A Voltage-time plot of the experiment would show a number of horizontal steps for a well-behaved surface. Each potential step would have its corresponding constituent formed. The final potential step for all substances corresponds to the reduction reaction and hydrogen ions are formed in the solution representing an end to the reaction beyond which no higher potential reduction process can occur. From the elapsed times at the various potential steps, information regarding the corrosion and tarnishing processes occurred in the environmental chamber could be deducted. The time taken for each voltage step and the number of coulombs of electrical charge required to complete the

reduction process at that particular voltage. The reduction voltage (at which the reduction of a particular chemical compound has occurred) can also be used to identify a compound whose characteristics reduction potential has already been established under the conditions of the test [36]. The graph of Voltage-time is shown in Figure 5-31.

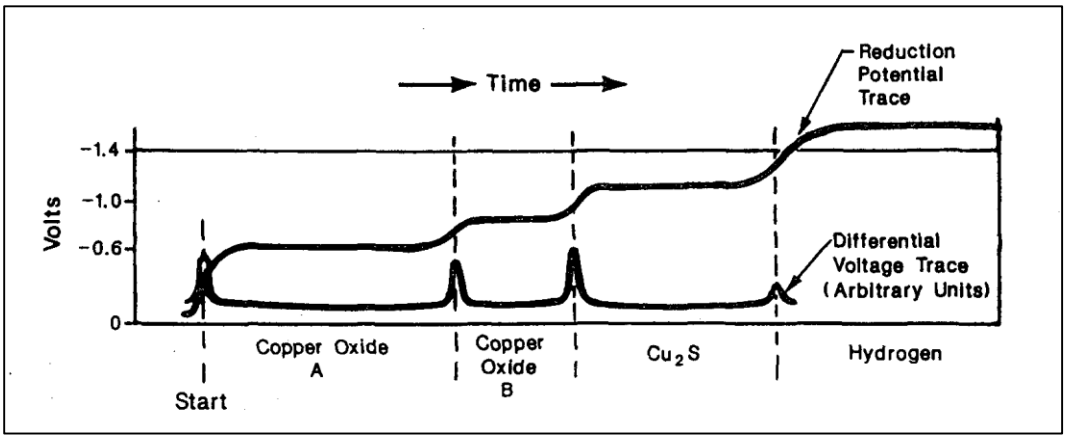

Figure 5-31 Reduction behavior of simple films on copper

(Image source: [36])

A current density of 0.05 milli-amperes per square centimeter of immersed metal is applied and the same current density is used to analyze the tarnished films. The current density may vary for thick films. The explanation of the procedure isn't covered here. The results of the coulometric reduction procedure can be expressed directly in terms of time (in seconds) required for the complete reduction process to occur at its particular voltage. The number of coulombs of electrical charge can be obtained by multiplying this time to the calculated current applied.

$$q = it$$

q= charge, mC,

i= current applied, mA and

t= time, s

For equivalent film thickness known,

$$T = \frac{itK}{a}$$

T=thickness, nm

i = current, mA;

t = time, s; a= area, cm^2

K= conversion factor

$$K = \frac{M * 10^4}{NFd}$$

where *d* = density of the substance being reduced, g/cm^2

Values of d, M and K for some common film constituents are listed in Table 5-1 [36]

Table 5-1 Factors for calculating mass or thickness of known films

Component	Density	Gram-Molecular Weight	Reduction Potential	K- Factor
Cu_2O	6	143.1	0.55-0.75	12.4
CuO	6.4	79.54	0.7-0.9	6.43
Cu_2S	5.6	159.1	1.0-1.15	14.7
Ag_2S	5.56	143.3	0	17.5
AgCl	7.32	247.8	0.82	26.7

5.2.2 A graph of Corrosion rate at various relative humidity values for Copper and Silver

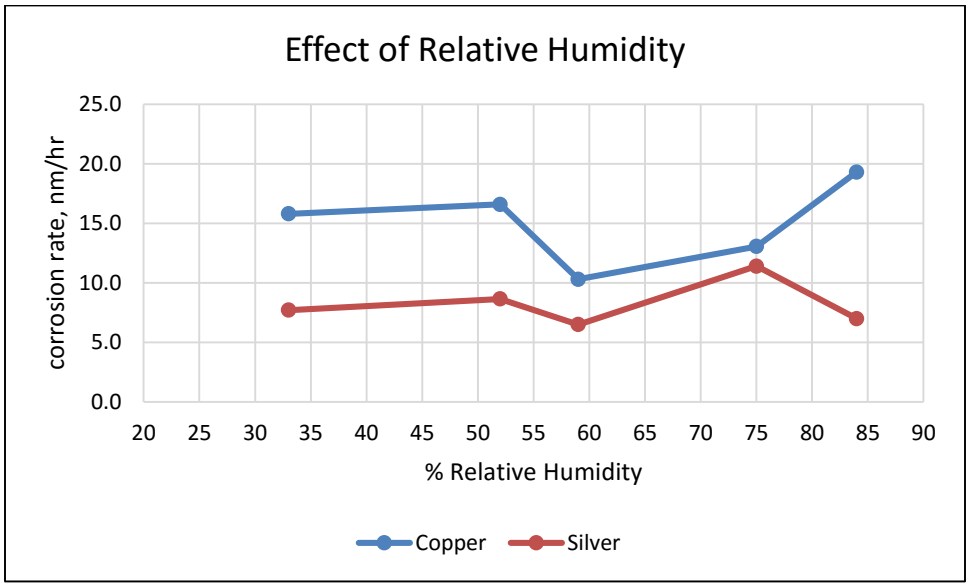

Figure 5-32 Corrosion of Coupons with respect to RH

The graph in Figure 5-32 shows the corrosion rate of copper and silver for corrosion coupon at various humidity levels. The coupons as they are not subjected to any dynamic heating resulted into the similar behavior of corrosion of copper and silver metals with changes in relative humidity levels. Yet, the corrosion for copper is higher the silver. This result is in line with the ASHRAE 2011 Gaseous and Particulate Contamination Guidelines for Data Centers where copper corrosion for coupon is higher than silver corrosion. If the results of this research are analyzed by the virtue of the corrosion rate value, then copper has tendency to corrode more than silver when the temperature surrounding it, i.e. the localized relative humidity remains constant.

5.2.3 Comparison between results of Thin Films and Coupons

Table 5-2 Comparison between Thin Films and Coupons

	%RH		Corrosion Rate, nm/hr	
			Coupon	**Thin Film**
#3 MgCl2	33	Cu	15.8	1.9
		Ag	7.7	3.7
#5 MgNO3	52	Cu	16.6	1.7
		Ag	8.6	3.3
#8 NH4NO3	59	Cu	10.3	1.8
		Ag	6.5	3.1
#4 NaCl	75	Cu	13.1	1.4
		Ag	11.4	2.4
#9 KCl	84	Cu	19.3	1.4
		Ag	7.0	3.5
#2 KNO3	91	Cu	X	1.9
		Ag	X	3.7

Here, X is results that is not available. The first experiment was conducted for 91% RH and corrosion coupons were not placed in that experiment.

The results of coulometric reduction of thin films are shown in Table 5-2. Based on the values of corrosion rates of thin films by the virtue of resistance, the results of coulometric reduction is not very meaningful and hence can be overlooked at the moment.

5.3 Psychrometric Chart

1. Copper Corrosion Rate

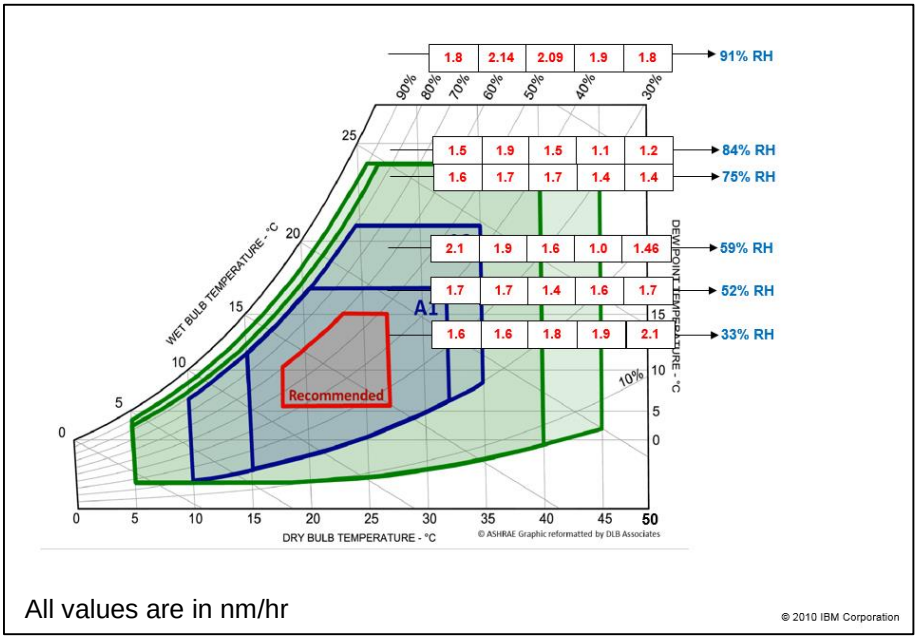

Figure 5-33 Psychrometric chart with Copper Corrosion Rate

From the results of plotted on psychrometric chart for the copper thin films, it is observed that the copper corrosion value increases with increasing in the dry bulb temperature till the relative humidity is 59%. At each temperature value, a constant current is supplied for 5 hours. At 75% and 84% RH, the copper corrosion rate increases from 30° C to 40° C and then reduces.

2. Silver Corrosion Rate

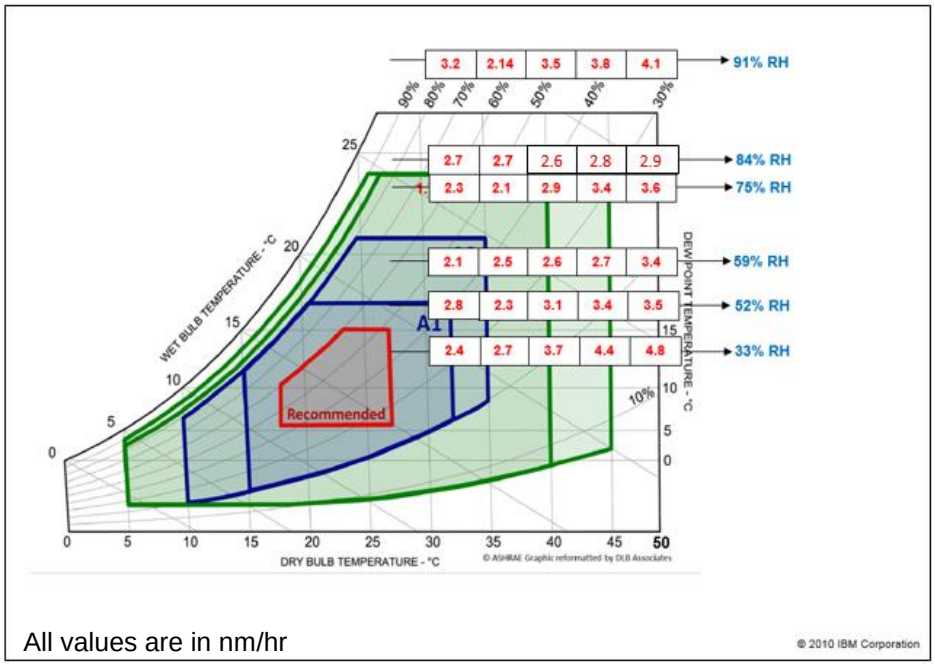

Figure 5-34 Psychrometric chart with Silver Corrosion Rate

From the results of plotted on psychrometric chart for the silver thin films, it is observed that the silver corrosion rate is almost 2.5 times higher than copper corrosion rate. The corrosion rate increases with increasing in the dry bulb temperature till the relative humidity is 59%. At 75% and 84% RH, the copper corrosion rate increases from 30 C to 40 C and then reduces.

5.4 3-Dimensional Corrosion Graphs

a. Copper Corrosion Rate

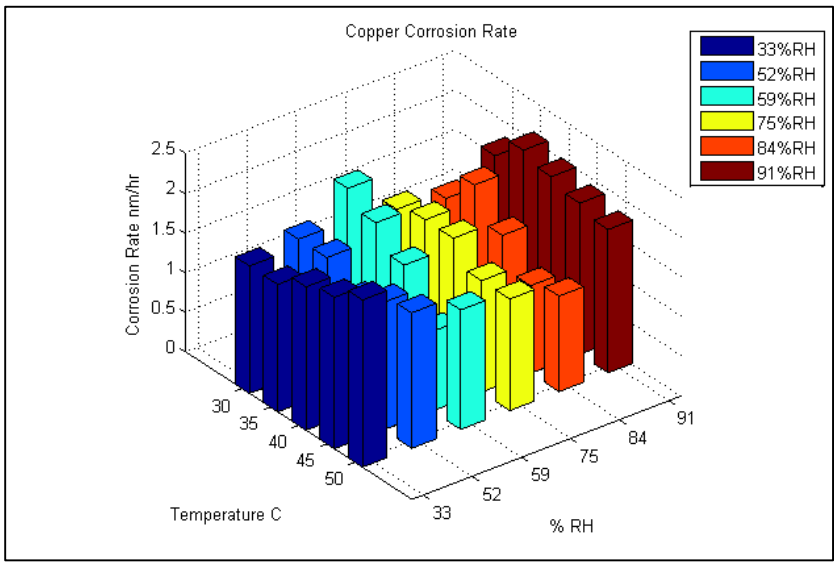

Figure 5-35 3-D Graph of Copper Corrosion Rate

b. Silver Corrosion Rate

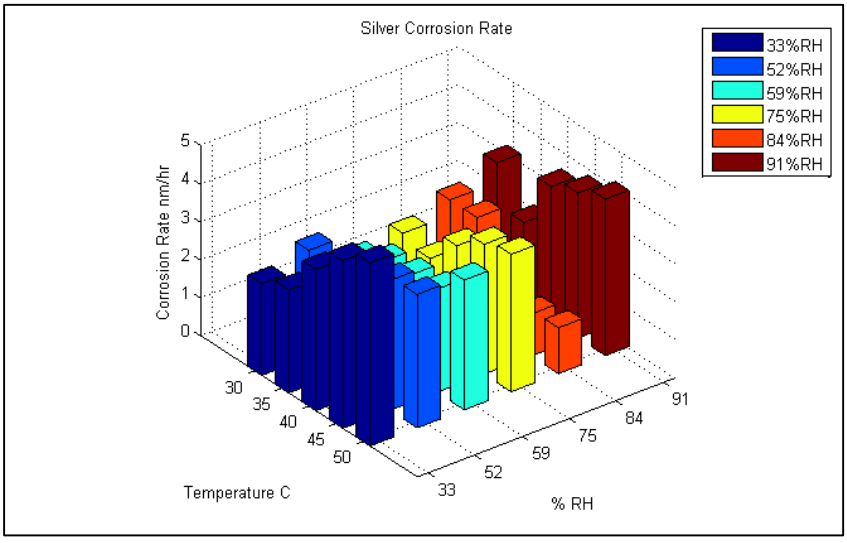

Figure 5-36 3-D Graph of Silver Corrosion Rate

The 3-dimensional graph of variation of corrosion rate with respect to temperature and relative humidity is shown in Figure 5-35 and Figure 5-36. The X-axis is the temperature and Y-axis is the relative humidity. Corrosion rate is the z-axis which comes out of the plane.

5.5 Conditions for Safe Operation

ASHRAE 2011 Gaseous and Particulate Contamination Guidelines For Data Centers recommending that gaseous contamination should be within the modified severity level G1 which meets are:

i. A copper reactivity rate of less than 300 Å/month and

ii. A silver reactivity rate of less than 200 Å/month

Any corrosion within this range is considered to be not prone to hardware failure but not safe. Care has to be taken to regularly clean and filter the server room and take precautionary measures to avoid further contamination.

Chapter 6

Conclusion and Future work

6.1 Conclusions

The corrosion rate for copper and silver has shown a regular behavior in most of the cases as we increase the temperature or relative humidity whereas for some data points it does not follow this trend. For thin films it is observed that silver corrosion rate is almost 2.5 times higher than copper corrosion rate in the field and the same behavior is seen from the experiments conducted in laboratory under continuous heating. The copper corrosion rate is observed to be very sensitive with changes in relative humidity. The behavior of silver was almost same in all conditions.

Silver corrosion is observed to be lesser than the copper corrosion for corrosion coupons under same conditions and this is very similar to the ASHRAE guidelines where the copper tends to corrode higher then silver. An analogy was derived from the results of thin films and corrosion coupons. For copper, the coupon gives higher corrosion when subjected to static heating as compared to dynamic heating. This means that the coupon showing higher corrosion has a tendency to corrode less when subjected to dynamic heating. Similarly, silver tends to corrode less when a constant temperature is maintained but corrodes more and faster when it has dynamic heating.

Also the corrosion rate of copper and silver is more sensitive due to Joule's heating or self-heating. The difference in the corrosion rate of thin film and coupon is due to different microstructure properties and surface finish.

6.2 Future Work

To understand the functional dependence of silver corrosion rate as it is believed to be affected by the synergy of different gases. To understand the chemistry of silver metal reacting in various conditions is important to have the clarity for silver corrosion rate. As the corrosion rate is believed to be affected by the synergy of gases, predicting the gaseous composition of the air using Gas Analyzers and simulating the same conditions in laboratory to understand the parameters affecting the corrosion rate in depth.

Validation of the experimental results for the corrosion rate can be done by performing CFD simulations to get a deeper insight. Also the gaseous contamination levels in a data center are a function of location and time of year. So to procure the real world data for corrosion from three different locations to find the levels of severity of the ambient air from different geographical locations can give an apple to apple comparision.

References

[1] "2008 ASHRAE Environmental Guidelines for Datacom Equipment," *ASHRAE TC 9.9 committee,* 2008.

[2] "http://www.koomey.com/post/8323374335".

[3] Prabjit, Singh; Levente, Klein; Dereje, Agonafer; Kanan, Pujara;, "Effect of Relative Humidity, Temperature and Gaseous and Particulate Contaminations on Information Technology Equipment Reliability," in *InterPACK/ICNMM*, San Francisco, 2015.

[4] *Thermal Guidelines for Data Processing Environments– Expanded Data Center Classes and Usage Guidance Whitepaper prepared by ASHRAE Technical Committee (TC) 9.9 Mission Critical Facilities, Technology Spaces, and Electronic Equipment,* 2011.

[5] *Thermal Guidelines for Data Processing Environments – Expanded Data Center Classes and Usage Guidance,* ASHRAE TC 9.9, 2011.

[6] "Impact of Air Filtration on the Energy and Indoor Air Quality of Economizer-based Data Centers in the PG&E Territory," Lawrence Berkeley National Laboratory, 2009.

[7] "Air-Side Economizer," Energy Star, [Online]. Available: www.energystar.gov/index.cfm?c=power_mgt.datacenter_efficiency_economizer_airside.

[8] "Reducing datacenter cost with an air economizer," Intel.

[9] P. Singh, P. Ruch, S. Saliba and C. Muller, "Characterization, Prevention and Removal of Particulate Matter on Printed Circuit Boards," IPC APEX, San Diego, Feb 2015.

[10] "Environmental conditions for process measurement and control systems: Airborne contamination," *ISA-The Instrumentation Systems, and Automation Society,* 3 Feb 1986.

[11] F. Haley, S. Prabjit, C. Levi, Z. Jing, A. Wallace, L. Dem, L. Jeffrey, L. Jane, Z. Solomon and L. Simon, "Testing Printed Circuit Boards for Creep Corrosion in Flowers of Sulfur Chamber".

[12] H. Fu, C. C., P. Singh, J. Zhang., A. Kurella, X. Chen, X. Jiang, J. Burlingame and S. Lee, "Investigation of Factors that Influence Creep Corrosion on Printed Circuit Boards," in *SMTA Pan Pacific Microelectronics Symposium*, Kauai, 14-16 Feb 2012.

[13] H. Fu, C. Chen, P. Singh, J. Zhang, A. Kurella, X. Chen, X. Jiang, J. Burlingame and S. Lee., "Investigation of Factors that Influence Creep Corrosion on Printed Circuit Boards Part 2,," in *SMTAI*, 2012.

[14] "Directive 2002/95/EC of the European Parliament and of the council of 27 Jan 2003 on the restriction of the," 2003.

[15] Y. Zhou and M. Pecht, "Reliability Assessment of Immersion Silver Finished Circuit Board Assemblies Using Clay Tests," in *Int'l Conf, on Reliability, Maintainability and Safety, ICRMC*, 2009.

[16] "Case Study of Printed Circuit Board Corrosion and Countermeasures"," in *NTT EAST Ota-ku, 144-0053* , Japan.

[17] D. W. Rice, P. Peterson, E. B. Rigby, P. B. P. Phipps, R. J. Cappell and Tremoureux, "Atmospheric Corrosion of Copper and Silver," *J. Electrochem. Soc.,,* pp. pg. 275-284, 1981.

[18] ASHRAE , "Contamination Whitepaper," ASHRAE , July 2009.

[19] "Particulate and Gaseous Contaminants in Datacom Environments (ASHRAE 2009b)," *ASHRAE whitepaper.*

[20] C. W. Grunewald, "Z. Phys. Chem., B40, 455," 1938.

[21] H. Sereda and G. P. J., "Metal Corrosion in the Atmosphere," ASTM Stp. No. 435, 326-59, 1968.

[22] W. H. J. Vernon, Trans. Faraday Soc.,, 23, 113 (1921); 23, 162 (1927); 27, 264 (1931); 29, 35 (1933) ; 31, 1668 (1935).

[23] W. E. Thomas and H. P. Campbelt, Holm Conference Proceedings, pp. 233-265, 1968.

[24] S. Mrowec and F. Z. A., "High Temperature Metallic Corrosion of Sulfur and its Compounds," The Electrochemical Society Softbound Proceedings Series,, Princeton, N.J., 1970.

[25] W. E. C. a. H. P. Thomas, in *Holm Conference Proceedings, pp. 233-265*, 1968.

[26] W. H. Abbott, in *IEEE Trans. Parts, Hybrids, Packag.,*, 1974.

[27] J. A. Lorenzen, in *Institute of Environmental Sciences Proceedings, pp. 110-114*, 1971.

[28] S. P. Sharma, in *This Journal, 125, 2005* , 1978.

[29] V. S. Benjamin, S. Michael, Z. K. Roumen, L. B. Gustavo, R. I. Rogelio, B. Monica Carrillo, N. Nicola Radnev, A. Mario Curiel, G. Navor Rosas and R. JoseMaría Bastidas, *Copper Corrosion by Atmospheric Pollutants in the Electronics Industry,* Hindawi Publishing Corporation, 2013.

[30] L. Veleva, B. Valdez, G. Lopez, L. Vargas and J. Flores, *Atmospheric corrosion of electro-electronics metals in urban desert simulated indoor environment,* 2008: Corrosion Engineering Science and Technology.

[31] J. F. Valdez and S. B. Flores, *Cabina de simulaci´on de corrosion para la industria electr´onica en interior,* Ingenieros, vol. 6, no 21,, 2003.

[32] M. Chris and C. Grant, "Changes Required for Protection of Today's Process Control Equipment," ISA Standard 71.04.

[33] R. Allen and M. Trzeciak, "Measuring Environmental Corrosivity," in *25th Holm Conference, Illinios Institute of Technology*, Chicago, 1979.

[34] P. J. Peterson, "Corrosion of Materials and Magnets," in *ASTM STP 1148*.

[35] T. V. Bagul, "Computational study of behavior of gas absorption in data ceter equipment and its effects on the rate of corrosion/contamination," UTA, Alington, 2014.

[36] S. J. Krumbein, B. Newell and V. Pascucci, "Monitoring Environmental Tests by Coulometric Reduction of Metallic Control Samples," Journal of Testing and Evaluation, 1989.

[37] H. H. Uhlig, The Corrosion Handbook, New York: John Wiley & Sons, Inc, 1948.

Biographical Information

Kanan Dinesh Pujara, has received her Bachelors of Engineering degree in Mechatronics Engineering from the Sardar Patel University, Gujarat, India. She has completed her Masters in Mechanical Engineering from the University of Texas at Arlington, US in December 2015.

Kanan's interest has always been in the field of Computational Fluid Dynamics, HVAC systems and Machine design. Her interest in this field got her the opportunity to work with one of the engineering giant, Larsen and Toubro, Bangalore-Baroda, India for 5 years working in the field of Computational Fluid Dynamics (CFD). Her research interests has always been into Fluid flow and Heat Transfer, Thermal Sciences and Design.

Coming from a business background, Kanan is always interested to be an entrepreneur. She would like to use her knowledge of the field of medical devices for the good of technology and to help mankind.